PCT/AU99/01052

AU99/01052

Patent Office
Canberra

I, KAY WARD, TEAM LEADER EXAMINATION SUPPORT AND SALES hereby certify that annexed is a true copy of the Provisional specification in connection with Application No. PP 7288 for a patent by THE UNIVERSITY OF QUEENSLAND filed on 25 November 1998.

WITNESS my hand this
Twenty-fourth day of December 1999

KAY WARD
TEAM LEADER EXAMINATION
SUPPORT AND SALES

PRIORITY DOCUMENT

SUBMITTED OR TRANSMITTED IN
COMPLIANCE WITH RULE 17.1(a) OR (b)

P/00/009
Regulation 3.2

AUSTRALIA

Patents Act 1990

PROVISIONAL SPECIFICATION

Invention Title: "IMMUNOSTIMULATORY DNA"

The invention is described in the following statement:

TITLE

"IMMUNOSTIMULATORY DNA"

FIELD OF THE INVENTION

THIS INVENTION relates to methods for identifying immunostimulatory DNA, which DNA stimulates cells of a mammalian immune system. This invention is also directed to methods for identifying agonists and antagonists of immunostimulatory DNA.

BACKGROUND OF THE INVENTION

A fundamental attribute of the mammalian immune system is the ability to distinguish self from non-self. This is most generally understood with regard to proteins and peptides, but it also applies to DNA.

In this regard, certain cells of the immune system such as B lymphocytes and macrophages are able to distinguish bacterial DNA from vertebrate and plant DNA (Messina *et al.*, 1991, J. Immunol. **147** 1759; Yamamoto *et al.*, 1992, Immunol. **36** 983; Stacey *et al.*, 1996, J. Immunol. **157** 2116; Klinman *et al.*, 1996, Proc. Natl. Acad. Sci. USA **93** 2879). That is, bacterial DNA can stimulate cells of the immune system, and as such is an example of "immunostimulatory DNA".

A core motif common to immunostimulatory DNA is the CpG dinucleotide motif, which appears to be central to the immunostimulatory capacity of DNA (Krieg *et al.*, 1995, Nature **374** 546). However, it is also clear that flanking sequence can be important, in that CpG sequences flanked by a cytosine (C) or guanine (G) nucleotide are less immunostimulatory (Krieg *et al.*, 1995, *supra*).

CpG sequences are relatively common in bacterial DNA, and are generally unmethylated. In contrast, CpG sequences occur less commonly in vertebrate DNA (about 25% of what would be expected based on random base utilization) and are generally methylated (Bird, 1987, Trends Genet. **3** 342; Bird, 1993, Cold Spring Harbor Symp. Quant. Biol. **58** 281), this characteristic being referred to as CpG suppression". Thus, by virtue of the presence of unmethylated CpG sequences, bacterial DNA can be distinguished by the immune system as being non-self, whereas "CpG suppressed" vertebrate sequences are treated as self. It should also be noted that unmethylated vertebrate CpG sequences tend to be flanked by C or G nucleotides, rendering them less immunostimulatory.

In B lymphocytes, CpG-containing DNA is a polyclonal activator of mitogenesis and cytokine production, and furthermore acts to block apoptosis, such as induced by anti-IgM treatment (Krieg *et al.*, 1995, *supra*; Messina *et al.*, 1991, *supra*; Sun *et al.*, 1997, J. Immunol. **159** 3119; Piseteky & Reich, 1993, Mol. Biol. Rep. **18** 217; Liang *et al.*, 1996, J. Clin. Invest. **98** 1119).

In macrophages and dendritic cells, and indirectly in NK cells, CpG-containing DNA partially mimics the action of bacterial lipopolysaccharide (LPS) (Chace *et al.*, 1997, Clin. Immunol. Immunopathol. **84** 185; Cowdery *et al.* 1996, J. Immunol. **156** 4570; Halpern *et al.*, 1996, Cell. Immunol. **167** 72; Sparwasser *et al.*, 1997, Eur. J. Immunol. **27** 1671; Sparwasser *et al.*, 1997, Nature **386** 336; Stacey *et* al., 1996, *supra*; Sweet

et al., 1998, J. Interferon Cytokine Res. **18** 263; Yamamoto *et al.*, 1992, *supra*). However, there are important differences between the effect of LPS and CpG-containing DNA. For example, although CpG DNA is as effective as LPS at inducing the transcription factor NF-κB and TNF-α mRNA, unlike LPS it is a poor inducer of interleukin 1 β (IL-1β) and does not, by itself, induce nitric oxide synthase (iNOS) (Stacey *et al.*, 1996, *supra*; Sweet *et al.*, 1998 *supra*). It has also been noted that CpG DNA is an excellent inducer of interleukin 12 (IL-12), and thereby acts to promote interferon gamma (IFN-γ) production in mixed cell cultures (Chace *et al.*, 1997, *supra*; Cowdery *et al.*, 1996, *supra*). IFN-γ in turn primes macrophages to respond to immunostimulatory DNA by expressing iNOS, thereby creating a self-amplifying loop with NK cells (Sweet *et al.*, 1998, *supra*).

The emerging consensus is that immune modulation by immunostimulatory DNA involves elicitation of IL-12 production by macrophages which thereby contributes to the polarization of T-lymphocyte responses towards an IFN-γ-producing T-helper 1 (Th1) phenotype (Carson & Raz, 1997, J. Exp. Med. **186** 1621; Chu *et al.*, 1997, J. Exp. Med. **186** 1623; Davis *et al.*, 1998, J. Immunol. **160** 870; Lipford *et al.*, 1997, Eur. J. Immunol. **27** 2340; Roman *et al.*, 1997, Nature Med. **3** 849; Weiner *et al.*, 1997, Proc. Natl. Acad. Sci. USA **94** 10833; Zimmerman *et al.*, 1998, J. Immunol. **160** 3627). As would be expected from the Th1 cytokines induced by immunostimulatory DNA, the immune response is typically Th1-like, and characterized by a predominance of IgG_{2a} antibody production and strong

CTL induction. In fact, it has been noted that CpG-containing DNA is a stronger Th1 adjuvant than complete Freunds adjuvant (Chu *et al.*, 1997, *supra*).

An important consequence of the response of the immune response to immunostimulatory DNA is that when such sequences are present in a plasmid vector, the plasmid vector can effectively act as an adjuvant. This has implications for vectors used in DNA vaccines, and it has been reported that CpG sequences are essential for effective DNA vaccination (Gregoriades, 1998, Pharm. Res. **15** 661, Klinman *et al.*, 1997, J. Immunol. **158** 3635; Sun *et al.*, 1988, J. Exp. Med. **187** 1145; Sato *et al.*, 1996, Science **273** 352). It will also be appreciated that an increasing number of studies have utilized synthetic oligonucleotides (ODN) which contain immunostimulatory CpG sequences as immunomodulators in their own right (Schwartz *et al.*, 1997, J. Clin. Invest. **100** 68; Wooldridge *et al.*, 1997, Blood **89** 2994; Kline *et al.*, 1998, J. Immunol. **160** 2555).

The limited mechanistic studies of how immunostimulatory DNA stimulates macrophages and B lymphocytes suggest that immunostimulatory DNA must be internalized. For example, chloroquine which interferes with endosomal function, blocks the actions of immunostimulatory DNA, but not the actions of LPS (MacFarlane & Manzel, 1998, J. Immunol. **160** 1122; Yi *et al.*, 1998, J. Immunol. **160** 4755). Thus, it has been postulated that cellular recognition of immunostimulatory DNA probably occurs within the cytoplasm or nucleus. Since single-stranded DNA can be

immunostimulatory, recognition might be achieved by an intracellular receptor which recognizes single-stranded immunostimulatory DNA in a CpG sequence-specific manner. The major known ssDNA-binding activity in eukaryotic cells is replication protein A (RPA).

RPA exists as a complex of three subunits:-

(i) a 70 kD subunit (RPA70 or RPA1) which contains two DNA-binding domains;

(ii) a 34 kD subunit (RPA34 or RPA2); and

(iii) a 14 kD subunit (RPA14 or RPA3).

RPA34 and RPA14 have been shown recently to form a separate DNA binding domain that may also interact with the C-terminus of RPA70.

The major functional role for RPA is as an indispensable player in normal cellular DNA replication, namely by being required for DNA strand separation and unwinding. (reviewed in Wold, 1997, Ann. Rev. Biochem. **66** 61). RPA also recognizes DNA damaged by agents such as UV light and cisplatin, and contributes to repair of damaged DNA (Burns *et al.*, 1996, J. Biol. Chem. **271** 11607; Patrick & Turchi, 1998, Biochemistry **37** 8808). Thus, the crucial role of RPA in general processes relating to cellular DNA replication and it's relative lack of sequence specificity, had rendered RPA an unlikely candidate as a sequence-specific receptor for CpG-containing immunostimulatory DNA (Wold, 1997, *supra*).

OBJECT OF THE INVENTION

Surprisingly, as a result of re-assessing the nucleotide

sequence specificity of the immune response to immunostimulatory DNA, the present inventors have identified RPA as the intracellular receptor for immunostimulatory DNA.

It is therefore an object of the invention to provide a method for the identification of immunostimulatory DNA.

SUMMARY OF THE INVENTION

In one aspect, the invention resides in a method of detecting immunostimulatory DNA, including the steps of:-

(i) combining isolated RPA with a sample suspected of containing immunostimulatory DNA;

(ii) forming a complex between said isolated RPA and said immunostimulatory DNA, if present in said sample; and

(iii) detecting said complex formed in step (ii).

It will be appreciated that the method of the invention provides a means whereby the immunostimulatory capacity of DNA can be assessed. As used herein, DNA includes single- or double-stranded DNA, single- or double-stranded synthetic oligonucleotides and plasmid DNA such as used in gene therapy or DNA vaccination. Also contemplated are analogs of DNA, particularly synthetic analogs such as phosphorothioate-modified oligonucleotides. It will be understood that the first aspect of the invention makes particular use of the discovery that RPA is the receptor for immunostimulatory DNA, and allows direct identification of immunostimulatory DNA by virtue of its ability to bind isolated RPA.

In this regard, the present inventors have identified three RPA

species hereinafter designated Band A and Band B and Band C respectively, which form complexes with immunostimulatory DNA. The proposed subunit composition of Bands A-C will be discussed in detail hereinafter.

Said isolated RPA may be recombinant RPA, RPA purified from a cellular source, or in the form of a nuclear or cytosolic extract. Recombinant RPA may be produced in bacteria, insect cells (e.g. by baculovirus expression in Sf9 cells) or in mammalian cells by techniques well known in the art, such as provided in Chapter 5 of CURRENT PROTOCOLS IN PROTEIN SCIENCE (Coligan *et al.*, Eds; John Wiley & Sons) which is herein incorporated by reference.

According to the above aspect, steps (ii) and (iii) may be performed using an Electrophoretic Mobility Shift Assay (EMSA) or solid phase binding assays. Appropriate solid phase assays include immobilizing either RPA or said sample to a solid matrix such as microtitre plate, BiaCore sensor chip, magnetic bead (e.g. DynaBead or BioMag bead) or synthetic polymer (e.g. sepharose) beads, and detecting formation of said complex on said solid matrix.

Preferably, steps (ii) and (iii) are performed using EMSA. EMSA involves formation of a complex between DNA and protein, in this case said protein being RPA present in a macrophage-derived nuclear or cytosolic extract, and electrophoretic separation of the DNA-protein complexes from non-complexed DNA. Preferably, separation is by non-denaturing polyacrylamide gel electrophoresis (PAGE). Less preferably,

agarose gel electrophoresis is used. Detection of RPA-containing complexes and non-complexed DNA is achieved by virtue of the DNA being associated with a label. Suitable labels include radionuclides or fluorescent labels such as TET, FAM or HEX. Preferably, the label is ^{32}P.

Preferably, EMSA includes a step whereby RPA-containing complexes are identified as supershifted complexes by addition of an anti-RPA antibody during formation of said complex. Such supershifted complexes have higher relative molecular weight than complexes in the absence of added antibody, and hence are readily discernible following size separation such as by PAGE. The particular advantage of this step is that the antibody provides a more specific means of identifying RPA-containing complexes.

Anti-RPA antibodies are readily available from commercial sources such as NeoMarkers and SeraLab. A suitable EMSA method may be found, for example, in Ross *et al.*, 1994, Oncogene **9** 121 which is herein incorporated by reference, and which forms the basis of a detailed description of an EMSA method applicable to the method of the invention as provided hereinafter.

In another aspect, the invention resides in a kit for detecting immunostimulatory DNA, said kit comprising:-

(i) isolated RPA; and

(ii) an RPA-specific antibody.

Preferably, the isolated RPA is recombinant synthetic RPA produced according the methods such as already described. It is envisaged

that different subunit compositions may be provided (e.g. comprising RPA70, RPA34, RPA14 and a 55 kD proteolytic product of RPA70). The kit may be applicable to EMSA or solid phase binding assays as previously discussed. In this regard, additional components may be provided such as pre-cast polyacrylamide gels, molecular size standards or RPA immobilized to beads, microtitre plates or other solid matrices. Furthermore, control reagents may be included such as a known immunostimulatory DNA standard, and a non-immunostimulatory DNA "negative control".

In yet another aspect, the invention resides in a method of detecting an immunostimulatory DNA including the steps of:-

(i) combining macrophage cells with a sample suspected of containing immunostimulatory DNA;

(ii) measuring a response by said macrophage cells to said immunostimulatory DNA, if present in said sample, said response selected from the group consisting of:-

(a) a cell-cycle arrest; and

(b) a reduction in CSF-1 receptor (CSF1-R) expression.

According to this aspect, the method of the invention provides a means whereby the immunostimulatory capacity of DNA can be assessed. As used herein, DNA includes single- or double-stranded DNA, including single- or double-stranded synthetic oligonucleotides, analogs thereof (such as phosphorothioate analogs), and plasmid DNA such as used in gene therapy or DNA vaccination.

Suitable cells applicable to this aspect are generally of the monocyte-macrophage lineage, and include bone marrow-derived macrophages (BMM), RAW264 cells and monoMac6 cells.

With regard to (a), cell cycle arrest is a specific response of macrophage cells to immunostimulatory DNA. The particular stage at which cell cycle arrests is at the G_1 to S-phase transition. Preferably, cell cycle status is measured by flow cytometric analysis of DNA content. Preferably, propidium iodide (PI) is used to stain total cellular DNA for flow cytometric analysis. However, it will be appreciated that other nucleic acid stains can be used, including acridine orange, YO-PRO-1, Hoechst 33358, and ethidium bromide.

Alternatively, cell cycle status is measured by methods which employ bromodeoxyuridine (BrdU) incorporation and detection of cells which have entered S-phase using an anti-BrdU antibody. Detection may be performed either by flow cytometric analysis (where the anti-BrdU antibody is conjugated to a fluorochrome such as fluorescein isothiocyanate (FITC), Cy5, (tetramethyl rhodamine iosothicyanate (TRITC), Texas Red or phycoerythrin (PE), for example), or by histochemical analysis (where the anti-BrdU antibody is conjugated to alkaline phosphatase or horseradish peroxidase, for example). It will also be apparent to one skilled in the art that flow cytometric analysis of DNA content can be combined with BrdU incorporation to provide a particularly sensitive bivariate analysis of cell cycle status. A detailed discussion of cell cycle analysis, DNA stains, fluorochromes, flow cytometry and methods of BrdU detection is provided

in Chapter 7 of PRACTICAL FLOW CYTOMETRY (3rd ED) by Howard M Shapiro (John Wiley & Sons), which is herein incorporated by reference.

With regard to (b), CSF-1R (also known as c-*fms*) is constitutively expressed at the cell surface of primary macrophages and a variety of monocyte-macrophage lineage cell lines such as RAW264 and monoMac6. Suitably, measurement of CSF-1R is performed using an anti-CSF-1R mAb. Preferably, the anti-CSF-1R antibody is detected by a secondary antibody conjugated to Cy5, or alternatively to another fluorochrome such as FITC, TRITC, PE or Texas Red. It is also envisaged that the anti-CSF-1R antibody may be directly conjugated to one of the abovementioned fluorochromes. Preferably, measurement of CSF-1R is performed by flow cytometric analysis of CSF-1R expression or by immunofluorescence microscopy, as will be described in detail hereinafter.

Other techniques for measuring cell surface CSF-1R expression include:-

(i) radioiodination of intact cells or membranes followed by immunoprecipitation (using anti-CSF-1R antibody); or

(ii) biotinylation of intact cells or membranes followed by affinity chromatography (using avidin-sepharose) and immunoblotting (using anti-CSF-1R antibody).

Strategies such as outlined in (i) and (ii) are well known in the art, and exemplary experimental protocols may be found in Chapter 3 of CURRENT PROTOCOLS IN PROTEIN SCIENCE (Coligan *et al.*, Eds; John

Wiley & Sons) which is herein incorporated by reference.

In a further aspect, the invention resides in a method of identifying an immunostimulatory DNA agonist or antagonist, including the steps of:-

(i) combining isolated RPA with immunostimulatory DNA and a sample suspected of containing an immunostimulatory DNA agonist or antagonist; and

(ii) determining whether or not a complex forms between said isolated RPA and said immunostimulatory DNA, an absence of said complex being indicative of said agonist or antagonist being present in said sample.

It will be appreciated that agonists and antagonists can be identified by their ability to compete with immunostimulatory DNA, and hence prevent formation of a complex between RPA and immunostimulatory DNA. Detection of the presence or absence of said complex may be according to the method of the first-mentioned aspect of the invention. However, it will also be understood that an antagonist cannot be distinguished from an agonist according to this method.

Agonists or antagonists so identified can subsequently be distinguished by a macrophage-based assay, such as according to the third-mentioned aspect of the invention. Another useful macrophage-based assay applicable in this regard utilizes RAW264a4 cells, which have a HIV LTR-luciferase construct stably integrated into their genome (Stacey *et al.*, 1996, *supra*; Sweet *et al.*, 1998, *supra*). These cells respond to immunostimulatory

DNA by expression of luciferase which can be readily measured in a semi-automated fashion. An example of a RAW264a4 luciferase assay will be provided in detail hereinafter.

The rationale for using a macrophage cell-based assay is that an agonist will cause macrophage cells to respond in a fashion similar to their response to immunostimulatory DNA. Conversely, antagonists will prevent a macrophage response to immunostimulatory DNA.

In light of the foregoing, it is envisaged that the methods of the invention may be used to identify immunostimulatory DNA, and agonists or antagonists thereof, in directed or high-throughput screens. Potential agonists and antagonists could be known compounds of unknown efficacy with respect to immunostimulation, the products of combinatorial chemistry, or be derived from natural sources. Such agonists and antagonists could become candidate drugs which mimic or block the effects of immunostimulatory DNA.

Based on the known properties of immunostimulatory DNA, novel agonists could be used as:-

(i) vaccine adjuvants;

(ii) immunotherapy for any form of cancer, allergic diseases (e.g. asthma);

(iii) immunotherapy for both chronic and acute inflammatory diseases and inflammatory autoimmune diseases (including but not restricted to systemic lupus erythematosus, arthritis, psoriasis, gingivitis,

sarcoidosis, multiple sclerosis, colitis and ileitis); and

(iv) activators of innate immune responses to protect against infection or to ameliorate symptoms of infection (e.g. septic shock).

Small molecule agonists or antagonists of immunostimulatory DNA may possess the particular advantage of displaying improved absorption by the oral route, compared to CpG-containing DNA for example, and be far more economical to produce on a commercial scale.

EXPERIMENTAL

1. ***MATERIALS AND METHODS***

1.1 *Luciferase reporter assays*

The RAW264a4 macrophage cell line, a stable transfectant with integrated HIV-1-LTR driving a luciferase reporter gene, was described previously (Sweet *et al.*, 1998, *supra*). Briefly, 2 x 10^5 cells were cultivated overnight in 24 well plates in 1 ml of medium overnight, then treated for the desired time with agonist, washed and extracted for luciferase activity determination using the Luciferase Reporter Gene kit from Boehringer-Mannheim and the 1450 Microbeta TRILUX plate luminometer.

1.2 *Cell proliferation/cell cycle and apoptosis measurements.*

Bone marrow-derived macrophages (BMM) were prepared by cultivation of CD1 outbred mouse femoral bone marrow cells in recombinant CSF-1 and harvested after 6-8 days as previously described (Stacey *et al.*, 1995, Mol. Cell Biol. **15** 3430, which is herein incorporated by reference). For cell proliferation assays, cells were cultivated in medium for the desired

time with or without CSF-1 and other additions, then a measure of the number of viable cells was obtained by incubation in the vital dye MTT as detailed previously (Stacey *et al.*, 1993, Immunol. Cell Biol. **71** 75). To assess cell cycle status, 10^7 cells preincubated with the desired stimuli were harvested, fixed and permeabilised by resuspension in 1 ml of PBS followed by addition of 3 ml of 95% ethanol and storage for at least 1 hr. Cells were washed in PBS, harvested incubated for 30 min in the dark with 2 ml of PBS containing RNaseA (0.2 mg/ml) and propidium iodide (40 µg/ml PI). Stained cells were analysed to determine the proportions in G_1, S, G_2 and M stages of the cell cycle using a Becton-Dickinson FACSCalibur flow cytometer. The proportion of apoptotic cells in similar incubations was assessed on the basis of exclusion of the vital dye propidium iodide (PI). Cells were incubated in 40 µg/ml PI in complete medium for 1.5 hrs at 37°C then analysed on a FACSCalibur flow cytometer.

1.3 *Immunofluorescence*

For direct visualisation, BMM were harvested, cultivated overnight on coverslips with the desired stimulus (e.g. with or without CSF-1) then treated or not with the appropriate stimulus and fixed with 4% paraformaldehyde in phosphate buffered saline. Fixed cells were permeabilised with 0.1% Triton X-100 in PBS for 5 min, washed 3 times with PBS, then 0.5% BSA in PBS for 15 min. Fixed and permeabilized cells were incubated with anti-*c-fms* monoclonal antibody (obtained from Dr J. Hamilton, University of Melbourne), for 90 mins, then Cy5-labelled $F(ab)_2$-goat anti-rat IgG second antibody (obtained from Serotec) with extensive

washing in phosphate buffered saline (PBS) between each step.

For FACS analysis, BMM were harvested at the desired time, fixed for 5 min in 4% formaldehyde in PBS, then incubated in the same succession of reagents as for direct visualisation. Staining was assessed using a FACSCalibur flow cytometer.

1.4 *Electrophoretic mobility shift assays*

Approximately 10^7 cells were lysed by hypotonic swelling followed by incubation in 0.1% NP40 detergent as described previously (Ross *et al.*, 1994, *supra*). Nuclei were separated from cytoplasm by centrifugation and the cytoplasmic extract was made up to a volume of 50 µl. Nuclear proteins were extracted from nuclei and made up to 50 µl in extraction buffer. Single-stranded or double-stranded oligonucleotide (DNA) probes obtained from Pacific Oligos (Brisbane) were end-labelled with ^{32}P, and incubated with 2 µg of cytoplasmic or nuclear protein extract for 30 minutes prior to separation on non-denaturing 7.5% polyacrylamide gel electrophoresis (PAGE). For supershift studies, monoclonal antibodies (mAb) against human RPA subunits RPA70 and RPA34 were provided by Dr. Bruce Stillman of Cold Spring Harbor Laboratory, NY USA, and were used directly as hybridoma supernatants. A rabbit heteroantiserum raised against purified human RPA (all three subunits), was a gift from Dr. Guiseppe Baldacci (Institut de Recherches sur Le Cancer, Villejuif, France). Irrelevant antiserum or hybridoma supernatant was added to control incubations.

For UV cross-linking experiments, EMSA gels were exposed

directly to UV transillumination and the positions of bands were identified by exposure of the wet gel to film. Bands were excised, extracted, and subjected to further separation by SDS-PAGE as described previously (Ross *et al.*, 1994, *supra*)

2. ***RESULTS***

2.1 *Determination of the optimal DNA structure recognised by murine macrophages*

In earlier studies the present inventors described a cell line assay for LPS in which the HIV-1-LTR driving luciferase enzyme expression is stably integrated into the DNA of the murine macrophage cell line RAW264 (Sweet & Hume, 1995, J. Inflamm. **45** 126). Addition of LPS to these cells (RAW264a4 cells) caused rapid activation of luciferase expression, peaking after around 2 hrs. This cell line also responds to plasmid DNA or activating oligonucleotides in a similar fashion. (Stacey *et al.*, 1996, *supra*; Sweet *et al.*, 1998, *supra*). Others (Lipford *et al.*, 1997, Eur. J. Immunol. **27** 3420) have claimed that different specific CpG DNA sequences can induce IL-12, but not TNF-α, in macrophages, with the implication that such "selective" oligonucleotides could harness therapeutic activities of CpG whilst avoiding toxic activities associated with induction of genes such as TNF-α. Most such studies have been based upon the use of phosphorothioate-modified oligonucleotides. Whilst of therapeutic relevance, such modification adds another variable since the phosphorothioate backbone is biologically active and may be toxic at high concentrations. We wished to ascertain whether differences in apparent

efficacy might relate to shifts in dose response curve that are not evident when a single concentration is examined. Such studies are expedited by the availability of an economical, rapid and convenient bioassay such as provided by RAW264a4 cells. FIG. 1A compares the relative activities of a range of published phosphodiester oligonucleotides with varying activities on the induction of luciferase activity in a4 cells. Examined at a single concentration, the AO-1 oligonucleotide is the most active phosphodiester oligonucleotide tested in macrophage assays, and is more active than the phosphodiester equivalent of the 1668 oligonucleotide (Ki *et al.*, 1996, J. Immunol. **157** 4918) and the IL12-p40 phosphorothioate ODN (described by Lipford *et al.*, 1997, *supra* as a weak activator that did not induce TNF-α). The difference between AO-1 and 1668 is simply an increase in length by adding terminal G nucleotides. ODN1668 and IL12p40 have the same core 10 bp sequence and differ in flanking bases on either side. Mutation of either one of the single flanking bases reduced the activity of the 1668 ODN. FIG. 1B shows that the difference in activity between ODN 1668 and IL12p40 is greater than is evident from a single concentration comparison, and results primarily from a change in dose response curve (i.e. a 5 fold shift in half-maximal concentration) and a lesser decrease in maximal response. Mutation in 1668 ODN of either of the flanking bases that distinguishes the two ODNs reduced the activity towards that of the less active IL12p40 ODN. The differences in efficacy of different ODNs are time independent; like the response to LPS, the response to each of the oligonucleotides reaches a peak after 2-3 hrs (FIG. 1C).

Activation of the HIV-1-LTR in the cell line assay in general parallels activation of TNF-α mRNA. Lipford *et al.* 1997, *supra* reported that the IL-12p40 ODN did not induce TNF-α mRNA or protein secretion, but the observation was made only at a single concentration (1 μM) and, as noted above, the ODN was a phosphorothioate derivative.

FIG. 2 compares the dose response curves for induction of TNF-α protein release from RAW264 macrophages. The conclusion is the same as for RAW264a4 cells. The difference in apparent efficacy of the different oligonucleotides simply reflects a shift in half-maximal activating concentration on the dose response curve and a smaller reduction in maximal response. This conclusion is important in terms of defining the mechanism of CpG DNA action, since it obviates any necessity to propose more than one recognition molecule or signalling pathway.

In summary, the results in the RAW264a4 cell assay, which measures NF-κB-dependent transcriptional activation, indicate that the sequence specificity of the response to ODNs is comparatively loose. The motif that is recognised may extend over up to 16 nucleotides. Different oligonucleotides have different dose response curves in the assay, and because the curves are very steep, assays at a single concentration can give a misleading impression as to the absolute requirement for sequence specificity.

2.2 *Cell cycle status, proliferation and apoptosis by bacterial DNA*

Induction of NF-κB-dependent transcription is one hallmark of the response of mammalian cells to DNA damage induced by a range of

genotoxic agents (Liu *et al.*, 1996, Nature **384** 273). Indeed, activation of the HIV-1-LTR has also been used as an indicator of such damage in fibroblasts (Miller *et al.*, 1997, Exp. Cell Res. **230** 9) and defective induction of NF-κB is associated with hypersensitivity to DNA damage-induced apoptosis (Jung *et al.*, 1998, Radiat. Res. **149** 596). We therefore considered whether the response to immunostimulatory DNA by macrophages might include changes in cell cycle progression. One of the hallmarks of the response to damaged DNA (e.g. caused by ionizing irradiation) is cell cycle arrest, or depending upon the extent of the insult, inhibition of apoptosis (see Liu *et al.*, 1998, *supra*). Others have shown that CpG DNA can prevent apoptosis induced in a B lymphoma line induced by anti-IgM (MacFarlane *et al.*, 1997, *supra*; Yi *et al.*, 1996, *supra*; Yi *et al.*, 1998, *supra*), but interpretation of these results is complicated by the fact that CpG DNA is itself a mitogen for B cells. We therefore examined whether treatment with immunostimulatory DNA affects cell cycle progression in murine bone marrow-derived macrophages which depend upon the macrophage-specific growth factor CSF-1, for survival and proliferation. BMMs starved of CSF-1 analysed following a propidium iodide based vital staining procedure showed decreased dye exclusion indicative of reduced cell membrane integrity. Bacterial plasmid DNA or immunostimulatory ODN prevented apoptosis completely, to the same extent as readdition of CSF-1 or LPS (FIG. 3). In contrast to CSF-1, neither plasmid DNA or ODN allowed cells to progress into the S and G2M phases of the cell cycle. In fact, like LPS (Hume *et al.*, Lymphokine Res. **6** 127) CpG-containing DNA also

caused almost complete inhibition of cell proliferation. This was evident by the reduction in the increase in cell number using a simple colorimetric assay for viable cells (data not shown). Cell cycle analysis using the FACS indicated that like LPS, CpG DNA caused a block to progression into S phase of the cell cycle (FIG. 4). These results indicate that both LPS and immunostimulatory DNA affect macrophages in a fashion similar to DNA damage in other cell types.

2.3 *CSF-1 receptor regulation in response to LPS and CpG DNA*

LPS has been shown previously to cause rapid down-regulation of CSF-1 binding to murine macrophages (Hume *et al.*, 1987, *supra*; Guilbert & Stanley, 1984, J. Immunol. Meth. **73** 17; Baccarini *et al.*, 1992, J. Immunol. **149** 2656). It was postulated by the present inventors that this response may underlie both the growth inhibition and survival described in the previous section. For this reason, the present inventors examined whether immunostimulatory DNA elicits CSF-1R down-regulation. FIG. 5A examines the expression of CSF-1 receptor on the surface of BMMs determined by immunofluorescence using a monoclonal antibody specific for the receptor encoded by the *c-fms* protooncogene (Sudo *et al.*, 1995, Oncogene **11** 2469). The specificity of the staining is evident from the rapid down-regulation that occurs in response to CSF-1). Both LPS and plasmid DNA or stimulatory ODN caused rapid disappearance of the CSF-1 receptor from the cell surface and its appearance in small cytoplasmic vesicles. These pictures also show that both treatments cause rapid polar spreading that is morphologically distinct from that elicited by CSF-1. At higher

magnification it is evident that both treatments apparently deplete the intracellular pool of *c-fms* that can be distinguished in the presumptive perinuclear Golgi regions and cause the appearance of extensive cytoplasmic vesiculation, which manifests as granularity under phase contrast.

The time course of *c-fms* down modulation can be measured more readily by FACS using anti-*c-fms* monoclonal antibody, which also gives single cell information. FIG. 5B compares the time course of down modulation by LPS and various immunostimulatory DNAs. At maximal concentrations of each agent all cells in the population show very rapid disappearance of CSF-1 receptors from the cell surface. The most rapid effect was obtained with plasmid DNA, which caused all cells to lose surface staining within 30 mins. LPS was next most rapid, followed by active ODN. In the latter case, the all-or-nothing nature of the responses is evident from the appearance of a bimodal distribution of surface staining at intermediate time points (FIG. 5B). In this assay, the CpG to GpC transversion of AO-1, and the methylated version of the ODN (AOM-1) which had barely detectable activity on luciferase activity in RAW264a4 cells, were also able to cause down-modulation but did not effect all cells and acted more slowly (FIG. 5C). The results indicate that down-modulation of *c-fms* in BMMs is a particularly sensitive assay for the response to CpG DNA and LPS, allowing detection of responses to ODNs that fail to elicit activated NF-κB-dependent transcription, although the same profile of sequence-dependent relative efficacy is evident.

2.4 *Identification of immunostimulatory DNA-binding proteins in macrophages*

Based upon the macrophage cell-based assays, the recognition molecule that mediates responses to immunostimulatory DNA should distinguish bacterial dsDNA from methylated or mammalian DNA. It need not be absolutely sequence specific for CpG motifs in single-stranded DNA but might be expected to follow the hierarchy of stimulatory potential identified in the bioassays described above.

One previous study has reported that all detectable single-stranded DNA binding activity in the cytoplasm of human or rodent cells extracted with mild detergent lysis is immunoreactive with antibodies directed against 70kD and/or 34kD subunits of RPA (Seroussi & Lavi, 1993, J. Biol. Chem. **268** 7147). FIG. 6A shows electrophoretic mobility shift assays (EMSA) of cytoplasmic and nuclear extracts produced from RAW264 cells compared with the fibroblast line 3T3. For comparison, the same extracts are probed with dsDNA probes having consensus sequences recognized by the macrophage-specific transcription factor PU.1, and the octamer transcription factors Oct-1 and Oct-2, both of which are expressed in macrophages (FIG. 6B). In each case, a low level of poly-dIC is present to reduce binding by a non-specific low affinity DNA binding protein that has been detected previously in mouse cells under similar conditions (Ross *et al.*, 1994, *supra*). The results show a complex set of bands that bind a single-stranded immunostimulatory ODN. In contrast to PU.1, and in even greater contrast to the octamer binding proteins (which are completely

nuclear restricted), the observed set of bands are not specifically enriched in the nuclear extracts, nor are they specifically excluded. In general, the gel system used herein resolves three major bands of binding activity in cytoplasmic extracts, referred to as Bands A, B and C in order of increasing electrophoretic mobility. A 4th single-stranded DNA binding band (B') is evident solely in nuclear extracts in this experiment, but was occasionally observed in cytoplasmic extracts.

The use of poly-dIC as a cold competitor was considered undesirable since it is also able to activate macrophages (Stacey *et al.*, 1996, *supra*). The present inventors therefore used sheared salmon-sperm DNA as a competitor. FIG. 6C shows a cold competition experiment in which increasing amounts of the DNA are added. In the extract shown there are 4 bands. Addition of relatively low concentrations of competitor reduced binding of all of the bands, with some selectivity for the B' nuclear band discussed above. The most stringent test of whether the cytoplasmic DNA-binding proteins are relevant to immunostimulation is whether they are also able to recognise plasmid DNA. FIG. 6D shows a cold-competition experiment in which the complex formed with activating ODN 1668 is cold-competed with plasmid DNA, with or without salmon sperm DNA. The faster migrating bands (including bands B and C) were effectively cold competed with plasmid DNA.

The present inventors next considered whether the major binding activities could distinguish between activating and non-activating ODNs. FIG. 7 contains a series of comparisons of non-activating and

activating ODNs. In FIG. 7A, the binding of ssDNA and ds DNA oligonucleotides is compared, in this case using the active ODN referred to previously as AAC-22 (Stacey *et al.*, 1996, *supra*). A series of independent extracts from RAW264 cells provided very similar patterns of binding, and despite the presence of the salmon sperm DNA, single-stranded and double-stranded activating ODN behaved identically. Because probe is present in excess, it is not possible to determine with assurance whether this binding involves recognition of non-annealed ssDNA. Cold competition with an excess of either ssAAC-22, or the ACC ODN which lacks immunostimulatory activity, provides evidence that the activity does bind ssDNA preferentially. Furthermore, where ssAAC-22 could completely cold-compete all the bands, the inactive ODN was unable to do so at a similar concentration, indicating that both ssDNA and dsDNA binding is sequence specific.

To extend these findings, the present inventors performed dose-dependent cold-competition experiments. Panel 7B provides evidence for greater relative binding activity by the activating oligonucleotide (AAC-22) under the conditions of the assay. Panel 7C shows an independent comparison of relative binding of a different set of ODNs with unrelated flanking sequences to AAC-22; the strongly activating AO-1, a non-activating GC transversion (NAO-1) and an oligonucleotide in which the core CpG motif is methylated. In each case the same set of complexes was formed with the labelled oligonucleotide. AO-1 was the most effective cold competitor regardless of whether it was competing with self, or with the less

active ODNs. Panel 7D confirms the findings in 7C with a comparative dose response curve for cold competition by each of the ODNs for binding of AO-1, indicating a 5-fold difference in apparent affinity. Finally, FIG. 7E shows a comparative cold competition for a strong (ODN1668) and weak (IL12p40) oligonucleotide that differ approximately 5-fold in relative activity in the RAW264a4 macrophage cell line assay (see above). Again, there was a 5-fold difference in the ability of the two ODNs to cold compete for binding to AO-1.

The affinity of RPA for ODN can be so high as to be effectively irreversible under the conditions of EMSA (Wold, 1997, *supra*). To determine whether this was the case for the cytoplasmic proteins in the present study, we examined the effectiveness of cold competitor added 15 minutes after the radiolabel (FIG. 8A). In this case, no release of labelled probe was observed even after a further 15 minutes of incubation for the slowest migrating band (Band A) whereas the faster migrating band B (C was not evident in this experiment) released the probe. Consistent with the reversibility of binding to the faster-migrating complexes, it is evident from FIG. 7 that these bands were always cold-competed more effectively than Band A.

The binding activity of RPA is known to be sensitive to alterations in ionic composition of the binding buffer, particularly the addition of magnesium (Wold, 1997, *supra*). We therefore examined whether addition of Mg^{2+} or increased levels of K^+ to the EMSA binding reaction altered complex formation. FIG. 8B shows that monovalent cations

increased the absolute binding activity of the abundant slow migrating complex. Conversely, Mg^{2+} above 2 mM caused a very substantial reduction in binding activity of the more slowly-migrating complex. These patterns are essentially consistent with binding activities of known forms of RPA (see discussion). Note that reduction/increase in binding activity of one of the three bands is not correlated with any change in other bands, suggesting that the alterations do not involve interconversion between different forms of DNA binding protein, but rather independent optimisation of the binding of each form.

To estimate the relative molecular weight of the ssDNA binding proteins, we performed a UV cross linking on RAW264 cell extracts. Results are shown in FIG. 9. The faster migrating band (band C) produced a single complex of around 55 kD. The slowest migrating band (Band A, which binds irreversibly) was not sufficiently resolved from the next band (band B) to give a clearly distinctive signal in preliminary experiments. Band B produced a doublet of around 70-75 kD with a very weak signal co-migrating with the 55 kD band produced from band C. When the total binding activity of the cytoplasmic extract was examined, it resolved into three major bands, the 55 kD band, the 70-75 kD doublet seen with band B and an additional major band of 30-35 kD. The 70-75 kD and 30-35 kD bands are consistent with identity as RPA1 and RPA2 subunits respectively. The 55 kD complex is consistent with a known truncated product of RPA70 (Wold, 1997, *supra*; Seroussi & Lavi, 1993, *supra*). Indeed, it was found that limited digestion of the extracts with trypsin led to the disappearance of

the slower migrating band A and appearance of a band that co-migrated with band C (not shown). Final confirmation of the identity of the three bands as forms of RPA was obtained using specific antisera. Because these antisera were raised against human proteins, we prepared an extract from the human macrophage line monoMac6 for comparison. Monoclonal antibody directed against human RPA70 or RPA34 completely supershifted the band B complex obtained from monoMac6 cells. Anti-RPA70 was inactive in mouse, but anti-RPA34 also shifted the faster migrating bands B&C. A heteroantiserum raised against purified human RPA also supershifted all the faster migrating bands (B&C) in both human and mouse (not shown). The specificity of these supershifts was confirmed by the absence of comparable changes in mobility with irrelevant monoclonal antibody or heteroantiserum at the same concentration.

3. ***DISCUSSION***

Based upon the results presented herein the present inventors have shown that RPA is the receptor for immunostimulatory DNA. The first evidence that a relatively non-specific ssDNA binding protein such as RPA is the receptor is based upon reassessment of the sequence specificity of the response. In essence, the response of macrophages to immunostimulatory ODNs is not absolutely determined by CpG core motifs, and actually appears to involve a relaxed activation motif of up to 16 bases wherein the primary effect of substitutions is to shift the dose-response curve. Because of the logistics of carrying out substitutions of all possible bases even within a short 6 base core motif, there have been limited studies

of sequence specificity of ODN responses, confused further by the effect of phosphorothioate backbone. The original report that a palindromic core was required for NK cell activation was not confirmed in studies on B cell mitogenesis (Krieg *et al.*, 1995, *supra*) and is not evident in any macrophage assays such as described herein.

The second line of evidence favouring RPA as receptor is that immunostimulatory DNAs induce in primary macrophages a range of changes that are characteristic of DNA damage in other cell types, including induction of NF-κB-dependent transcription and arrest of the cell cycle in G1. There is overwhelming evidence that RPA is a recognition molecule in several forms of DNA damage (Wold, 1997, *supra*). The present inventors have introduced novel cell-based assays for identifying immunostimulatory DNA: the rapid down-regulation of the CSF-1 receptor (*c-fms*); and prevention of cell cycle progression from G_1 to S phase.

The former reflects a massive increase in vesicle trafficking that occurs in stimulated macrophages and can be seen in rapid polar spreading of the stimulated cells on the substratum (not shown). The down-modulation is specific to the CSF-1 receptor in that the complement receptor (CD11b) and the macrophage-specific F4/80 antigen were not down-modulated in the same time frame (data not shown). It may also be that down modulation generates some form of stimulation via the CSF-1 receptor that is, in turn, connected to the anti-apoptotic response to both DNA and LPS. Low amounts of the receptor ligand, CSF-1 itself, can maintain viability of macrophages without triggering cell cycle progression (Roth & Stanley,

1992, Curr. Top. Microbiol. Immunol. **181** 141). Regardless of the causal relationship, and the mechanism of selective down-modulation, disappearance of *c-fms* provides an even more rapid and sensitive assay for immunostimulatory ODNs (and LPS) than the RAW264a4 assay of NF-κB-dependent transcription. The key finding arising from the use of this assay was that even ODNs such as NAO-1 and AOM-1 lacking the CpG core motif have detectable activity, albeit greatly-reduced, so a putative receptor need not have absolute DNA-binding specificity.

Thirdly, complementing the evidence that the sequence specificity of the biological response to ODNs is relatively relaxed, and even that the core CpG is not absolutely required, we show that RPA has sequence specificity for binding to DNA which correlates with relative biological efficacy in macrophages. RPA can distinguish bacterial from eukaryotic DNA, methylated from non-methylated plasmid DNA, activating from non-activating or methylated ODN, and ODN with subtly differing activity in the RAW264a4 assay (FIG. 6). RPA has been reported previously to have a 50-fold selective affinity for poly-pyrimidines as opposed to poly-purines (Wold, 1997, *supra*). Solution of the crystal structure of RPA70 complexed with an oligo-dC 8mer (Bochkarev *et al.*, 1997, Nature **385** 176) revealed a core binding site comprising the two ssDNA-binding domains in asymmetric conformation. Each ssDNA binding domain contacts 3 nucleotides, and the space between the two domains is bridged by two nucleotides. Both domains form multiple hydrogen bonds with all the DNA bases, implying potential for DNA-sequence-specific binding. The two

nucleotides that span the gap between the two ssDNA-binding domains make 6 independent hydrogen bonds with the protein, including 4 with the bases. The hydrogen bonds with these nucleotides are the same as would be formed in a base pair, involving O2 and N4 in each case. Given that the critical CpG is centred in the optimal sequence for immunostimulatory oligonucleotides, we hypothesise that the active CpG would form the two spanning nucleotides in the active complex with RPA and that the asymmetry of the two ssDNA binding domains in the complex could explain the asymmetry of the optimal immunostimulatory sequence RRCGYY. Further molecular modelling studies may provide insight into the possible effect of methylation of a C4 base in this proposed structure and the possible effect of contacts with the two bridging bases on the conformation of RPA70. Of course, as discussed below, the full complex with RPA also involves contact with RPA34, which could explain the more extended 16bp optimal motif indicated by the biological and DNA binding data. Thus, CpG sequence specificity and the reduced affinity for ODNs containing methylated C is entirely conceivable based upon the structure of RPA70.

The final evidence supporting the identity of RPA as the receptor is that it is abundant in the cytoplasm. Furthermore, there is no other detectable candidate receptor for DNA under our conditions of assay. In the cell fractionations shown in FIG. 1. A nuclear protein of comparable size to RPA, Oct1, was completely restricted to the nuclear fraction under similar conditions. A complex as large as RPA is probably not expelled from the nucleus under the conditions of mild cell lysis with NP-40 when other

nuclear proteins are retained. The location of RPA in the nucleus has been inferred based upon immunohistochemical localisation. However, there are contrary published data obtained from experiments using antibodies against different subunits; RPA14 was clearly detected in the cytoplasm (Wold, 1997, supra). Immunocytochemistry may give a false impression based upon the particular concentration of protein in the nucleus, leakage or selective destruction of antigen under the conditions of immunohistochemical localisation, or obscuring of antigenic epitopes in specific complexes of cytoplasmic RPA with other proteins (see below).

An important aspect of the work presented herein is the identification of at least three forms of RPA in macrophages and B cells. The UV cross-linking indicates that band A (in the mouse) contains both RPA 70 and RPA34, and that both subunits contact DNA. As noted in the introduction, RPA is known to undergo a conformational change upon binding of ssDNA. Initial binding of RPA is proposed to involve the approximate 8 base "footprint" seen in the 3D structure (Wold, 1997, *supra*) and to be relatively low affinity. Interactions between the RPA 34 and RPA14 subunits (also known as RPA2 and RPA3 respectively), which have independent ssDNA binding activity and the C-terminus of RPA70 (RPA1; Wold, 1997, *supra*) are required for transition to a high affinity irreversible binding state. Based upon the irreversibility of binding, the UV cross-linking and the inhibitory effect of Mg^{2+} (which is known to affect the conformational change in RPA) the present inventors propose that band A is the end-stage high affinity conformation of RPA. The conformation difference may explain

why Band A did not react with the particular anti-RPA antibodies available to us. Others (Seroussi & Lavi, 1993, *supra*) have found that the slowest migrating RPA band was bound by a different anti-RPA70 antibody which failed to recognize the faster migrating band(s) containing proteolytically cleaved RPA.

In the band B complex in FIG. 9, which can be cold competed by oligonucleotide added after binding of label only the 70kD RPA subunit appears to be in sufficiently close proximity to the ODN to permit UV cross-linking, but the complex is supershifted by anti-RPA34 antibody. One basis for the difference between RPA in band A and band B would be the phosphorylation of RPA 34 which is known to be occur upon DNA binding (Wold, 1997, *supra*) and might conceivably alter subsequent binding activity so that the high affinity complex involving contact with RPA34 cannot be formed. Band C, the complex containing the 55kD putative proteolytic cleavage product of RPA70 also showed no evidence of DNA contact with RPA 34. Initially, band C was observed inconsistently in macrophage extracts. Others have suggested that RPA70 cleavage may occur following cell extraction as an explanation for inconsistent identification of a presumed equivalent of our band C (Seroussi & Lavi, 1993, *supra*). However, the present inventors found that when extracts are prepared fresh and the incubation is carried out with added calcium, the level of band C in cytoplasmic extracts is consistent and reproducible (not shown). Accordingly, it has been concluded that band C is normally present in macrophages and represents a novel functional form of RPA.

In summary, the present inventors have provided evidence that there are several forms of RPA in macrophages, one or all of which have characteristics consistent with identity as the cytoplasmic receptor for immunostimulatory DNA. This conclusion is based upon the sub-cellular location of RPA, the binding specificity of RPA and the nature of the biological response to immunostimulatory DNA. A fundamental understanding of the recognition of immunostimulatory DNA by different forms of RPA should permit a more rational structure-function approach to optimising immunostimulatory DNA as a therapeutic agent.

FIGURE LEGENDS

FIG. 1

Effect of various oligonucleotides on luciferase activity in RAW264a4 cells. The indicator RAW264a4 cells with integrated HIV-LTR-luciferase construct were cultivated with the indicated oligonucleotides (defined in Materials and Methods) at the concentrations shown. After 2 hrs, or the indicated time in panel C, they were washed with PBS, lysed and luciferase activity was determined. In panel A and B the luciferase activity of control cells is normalised to a value of 1. Results are the average of triplicate determinations. Panel C, RLA is relative luciferase activity.

FIG. 2

Effect of oligonucleotides on TNF-α secretion. RAW264 cells (5×10^5 in 0.5 ml in a 24 well plate) were incubated with the oligonucleotides shown or with LPS as a positive control at the concentrations indicated for 18 hrs. The supernatants were harvested and the level of TNF-α secretion was assessed by ELISA. Results are the average of duplicates.

FIG. 3

Uptake of propidium iodide as an assay of DNA action. 10^6 BMM were harvested, washed and replated for 24 hrs in the presence of CSF-1, or in its absence (lower three panels). As indicated, *E. coli* genomic DNA (20 µg/ml) or LPS (100 ng/ml) was added. After 24 hrs, propidium iodide was added for 1.5 hrs as described in Materials and Methods. The FACS analysis plots fluorescence (vertical axis) against forward light scatter (an indicator of cell size). Cells in the R2 region of the profile are assessed as

having taken up propidium iodide and therefore are non viable. Note the at CSF-1, DNA and LPS all repress the appearance of these cells and also maintain a larger average (indicated by the right shift on the horizontal axis).

FIG. 4

LPS and bacterial DNA cause cell cycle arrest in proliferating macrophages. BMM ($5x10^6$) were incubated in 10^4 U/ml CSF-1 with addition of LPS (100 ng/ml) or *E. coli* genomic DNA (20 µg/ml) as indicated for 24 hrs. They were then permeabilized and stained for DNA content using propidium iodide as described in Materials and methods. Cells are ascribed a position in G_1, G_2M or S phase based upon 2N, 4N or intermediate DNA content respectively as indicated.

FIG. 5

Down modulation of c-fms surface receptor expression in bone marrow-derived macrophages. A. Bone marrow-derived macrophages were harvested, washed and replated on glass cover slips in the presence or absence of 10^4 U/ml CSF-1 overnight. CSF-1-starved cells were incubated with CSF-1, *E. coli* genomic DNA (20 µg/ml) or LPS (100 ng/ml) as indicated, the fixed for immunofluorescence localisation of *c-fms* antigen as described in Materials and Methods. Note the high level of surface *c-fms* expression in CSF-1 starved cells, which is rapidly down-modulated in response to CSF-1, DNA or LPS. B. FACS profiles of c-*fms* down modulation. Bone marrow-derived macrophages were starved of CSF-1 overnight, washed, and incubated with the oligonucleotides (20 µg/ml), LPS (100 ng/ml), *E. coli* genomic DNA (20 µg/ml) or CSF-1 (10^4 U/ml) for the

times indicated. After preincubation, fixation and immunostaining for c-*fms* antigen, cells were analysed on the FACS as shown. To allow convenient comparison on the vertical scale, the zero time control is reproduced in each column.

FIG. 6

Electrophoretic mobility shift analysis of location and specificity of ssDNA binding activity in various extracts. Radiolabelled single-stranded (AO-1) or double-stranded (PU-1, the PU box recognition sequence or Octamer; see Materials and Methods) were incubated with 2 µg of cytoplasmic (C) or nuclear (N) extracts in a binding buffer containing 12% glycerol, 20 mM HEPES (pH 7.9) plus 0.5 mM dithiothreitol, 2 mM EDTA, 40 mM KCl and 20 µg/ml sheared salmon sperm DNA. Extracts were then separated on non-denaturing 7.5% PAGE and exposed to autoradiographic film. The unbound probe has been run off the end to increase resolution of the protein bands. Panel A demonstrates the compartmentation of binding activity for ssAO-1 compared to well documented targets for dsDNA binding proteins in macrophages; PU.1 and Oct-1. The abundant band towards the bottom of the gel in both the PU.1 tracks (Panel A) has been shown previously to be PU.1, whilst the abundant nuclear band in the Oct tracks is Oct-1. Panel B compares the distribution of activities in RAW264 and NIH-3T3 fibroblasts. In both panels A and B the cold competitor is 20 µg/ml of sheared salmon sperm DNA. Panel C shows cytoplasmic extracts of RAW264 cells incubated with labelled ssAO-1 ODN. Various amounts of salmon sperm DNA are used as a cold competitor DNA. Note there is some selective loss

of the B' band at 0.2 µg of added cold competitor (20 µg/ml). In Panel D RAW264 cytoplasmic extracts were incubated with labeled immunostimulatory ssODN probe (M12=ATCCATAACGTTCCAGAAGCTG) together with plasmid DNA (the reporter plasmid pGL3C) in excess (fold-excess on a µg per µg basis) as indicated. Note the selective release of the lower band (band C) which has resolved slightly further in this particular experiment compared to panels A-C.

FIG. 7

Electrophoretic mobility shift analysis of sequence specificity of ssDNA binding activity. RAW264 cytoplasmic extracts were incubated with radiolabelled probes as indicated and separated on 7.5% non-denaturing PAGE. Buffer conditions were changed in different experiments to optimise visualisation of particular bands as indicated. Panel A compares the binding of RAW264 cytoplasmic proteins to single stranded or double-stranded immunostimulatory ODN AAC-22. Binding buffer is the as the nuclear extract buffer D and to avoid loss of dsDNA binding activities, no cold competitor was added. Four independent extracts of RAW264 (#1 to #4) show the same pattern of binding and the pattern is similar whether the probe is single-stranded (left panel) or double-stranded (right panel). Cold competition with single-stranded AAC-22, reveals that a 125-fold excess of self ODN completely prevents binding of both ss and ds-AAC-22, whereas the same amount of ss non-stimulatory ACC-22 failed to prevent significant binding of ss or dsAAC-22. Panel B shows quantitative cold-competition of binding of ss stimulatory ODN AAC-22 with cold self ODN or non-stimulatory

ACC-22 ODN. Note that there is approximately 4-fold difference in apparent relative affinity for stimulatory compared to non-stimulatory ODN. Binding buffer is also Buffer D. Panel C compares a different of ODNs using a separate RAW264 cytoplasmic extract, in this case band C (the lower band) is particularly abundant. Labelled probes are the immunostimulatory ODN AO-1 and the non-stimulatory GC transversion NAO-1 or the methylated form AOM-1. Note that in each case the pattern of binding is the same, but regardless of which ODN is labelled, AO-1 is the more effective cold-competitor. Binding buffer is the same as in FIG. 6, without cold competitor. This pattern is confirmed independently in panel D, with a separate RAW264 extract and AO-1 labelled as indicated. In this case, salmon sperm DNA was added (20 µg/ml) but does not alter the pattern of relative binding activity. Note that AO-1 is at least 5 fold more effective as cold competitor than either NAO-1 or AOM-1. In Panel E, the labelled probe is again AO-1 and the cold competitors are a separate immunostimulatory ODN (1668) and the weak activator IL-12p40. Note that a 10-fold excess of 1668 reduces binding to a similar extent to a 50-fold excess of IL-12p40 ODN. Binding buffer in this case contains 10 mM KCl, 5 mM $MgCl_2$ and 50 mM $CaCl_2$ to optimise detection of band C.

FIG. 8

Characteristics of the binding of ssDNA by RAW264 cytoplasmic proteins. Panel A shows a further independent confirmation of the ability of stimulatory ODN (AO-1) to cold-compete approximately 5-fold more effectively than non-stimulatory ODN, NAO-1. Binding buffer is the same as

in FIG. 6 with 20 µg/ml salmon sperm DNA as competitor. In the right panel, the labelled ODN was allowed to preincubate with cytoplasmic extract for 15 mins at room temperature prior to addition of cold competitor. Note that the faster migrating band is still competed but no reduction in the slower band (band A) is evident. Panel B examines the effect of changing the ion composition of the binding buffer. In each case the buffer is the and incubations are carried out in 20 mM HEPES buffer pH 7.9, varying only by additions of $MgCl_2$ or KCl as indicated. Note that binding of band A, the slower band, is increased by KCl and decreased by $MgCl_2$. Note also that the middle band, band B, is detected most readily in the presence of $MgCl_2$ and the absence of KCl.

FIG. 9

Primary gel shifts were carried out in binding buffer as in FIG. 6 and UV cross-linked *in situ* as described in Materials and Methods. The relevant bands were located, excised, extracted and re-run on SDS-PAGE with molecular weight standards as indicated. Bands and UV cross-link times are indicated.

FIG. 10

Cytoplasmic extracts were prepared from RAW264 cells and from the human macrophage cell line MonoMac6. Prior to addition of labeled ODN, the cytoplasmic extracts were incubated for 10 mins in irrelevant monoclonal antibody, anti-RPA34 or anti-RPA70 monoclonal antibody. Note that anti-RPA34 generates a new supershifted complex and completely represses the formation of the faster-migrating complexes. Anti-RPA70 abolishes the

formation of the faster-migrating complexes in the human line only, but does not generate a super-shifted band. Binding buffer in this case contained 20 mM HEPES pH 7.5, 140 mM KCl, 13 mM NaCl, 5 mM $MgCl_2$ and 20 µg/ml salmon sperm DNA.

DATED this twenty-fifth day of November 1998.

THE UNIVERSITY OF QUEENSLAND,

By their Patent Attorneys,

FISHER ADAMS KELLY.

FIGURE 1A

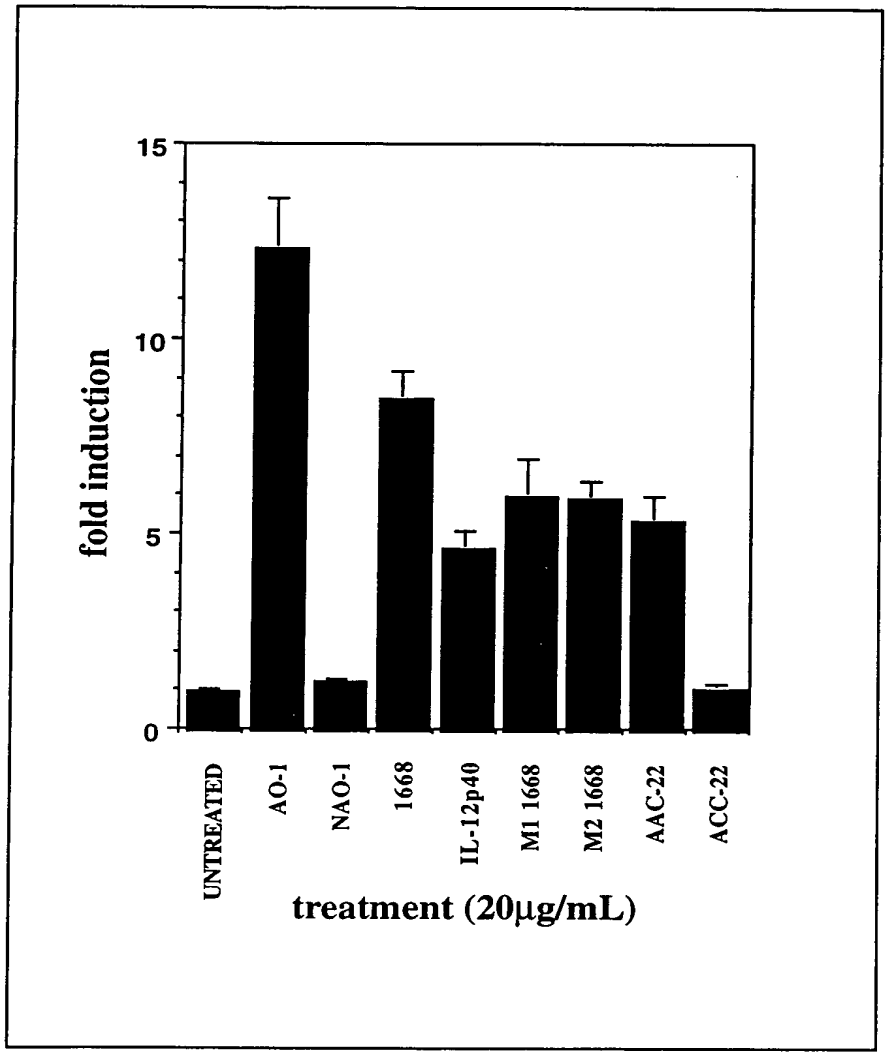
15
10
5
0
fold induction
UNTREATED
AO-1
NAO-1
1668
IL-12p40
M1 1668
M2 1668
AAC-22
ACC-22
treatment (20µg/mL)

FIGURE 1B

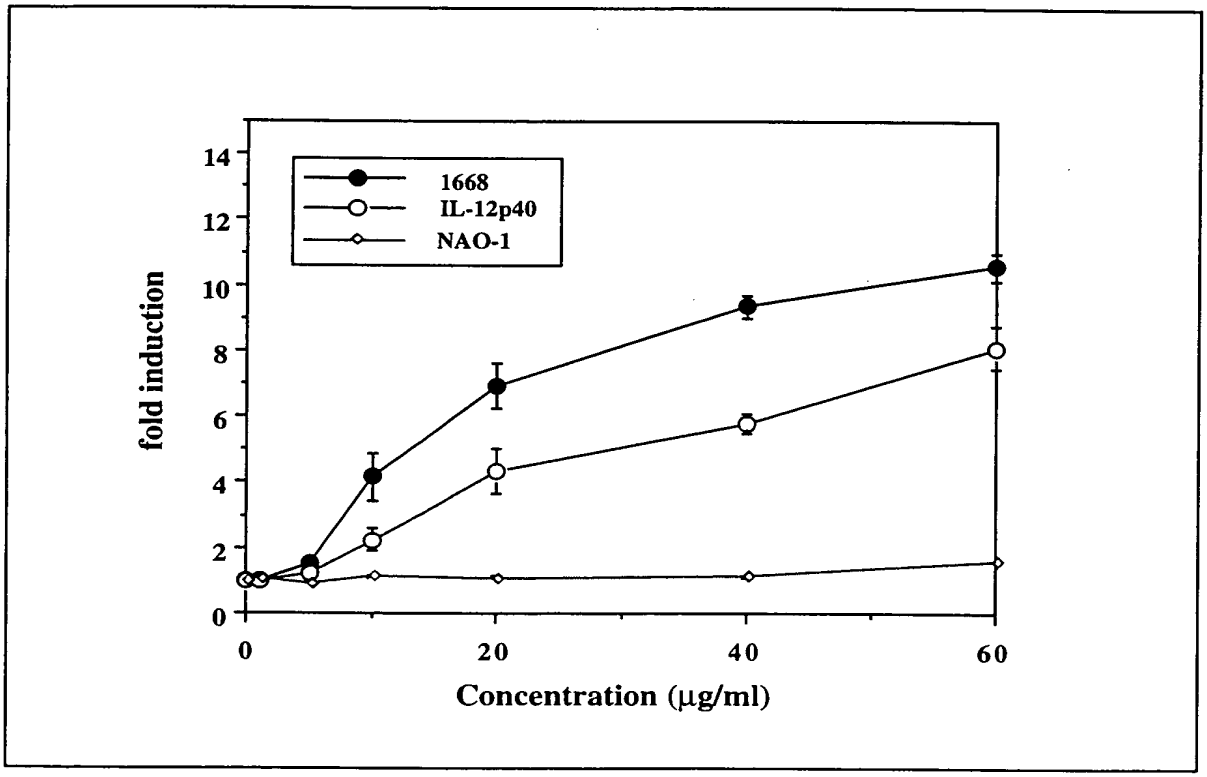
1668
IL-12p40
NAO-1
fold induction
0
2
4
6
8
10
12
14
0
20
40
60
Concentration (μg/ml)

FIGURE 1C

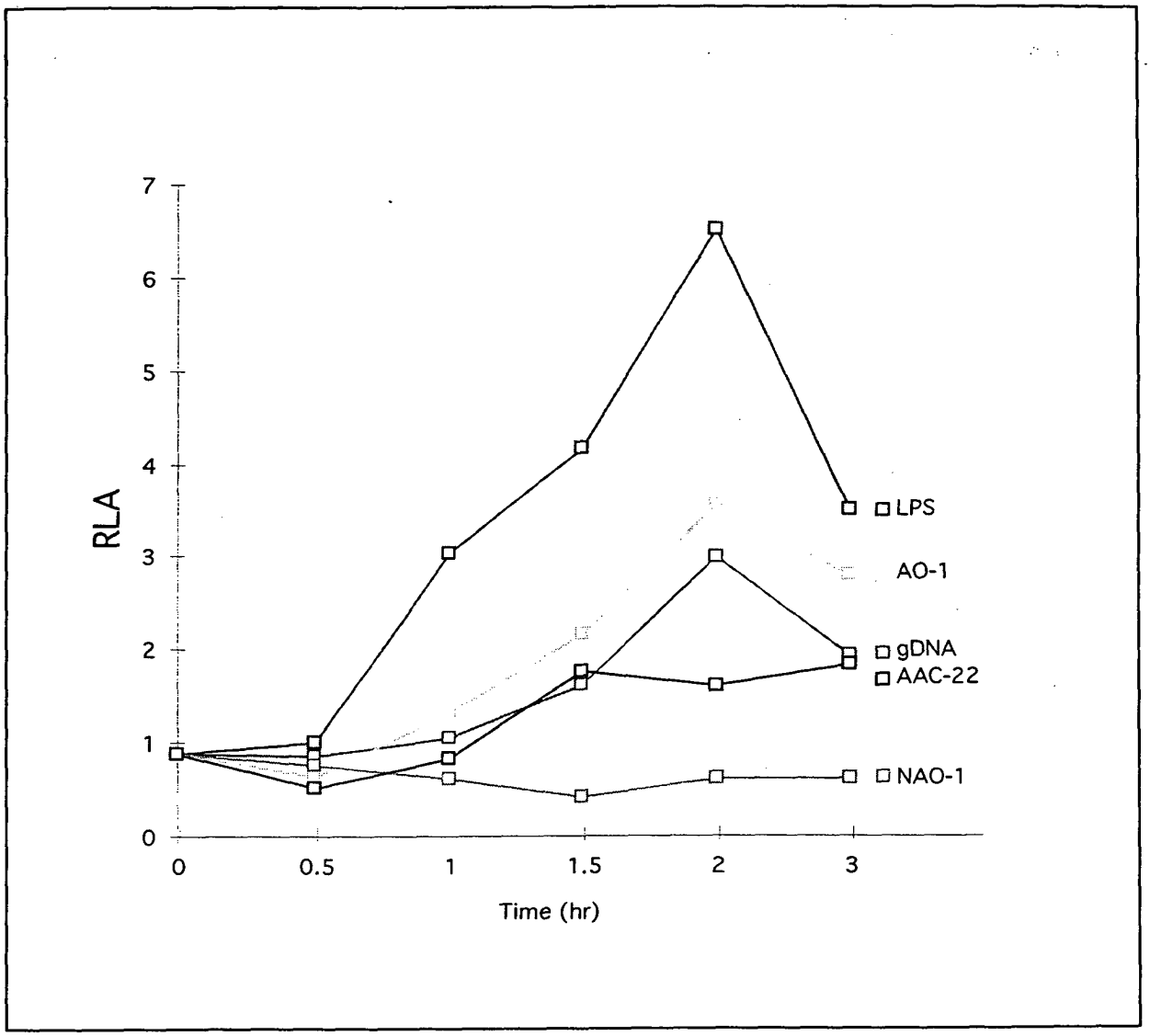

FIGURE 2

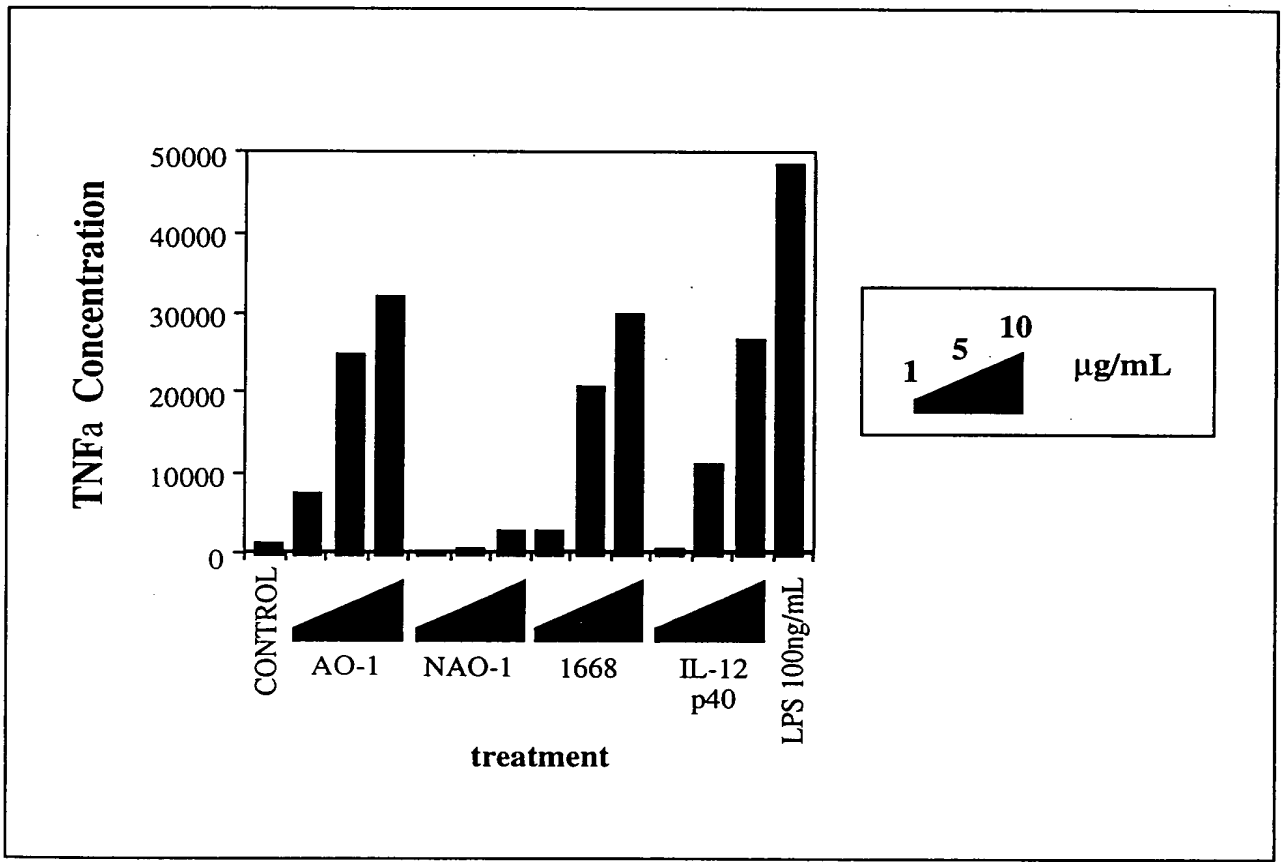
TNFa Concentration
50000
40000
30000
20000
10000
0
CONTROL
AO-1
NAO-1
1668
IL-12 p40
LPS 100ng/mL
treatment
1
5
10
µg/mL

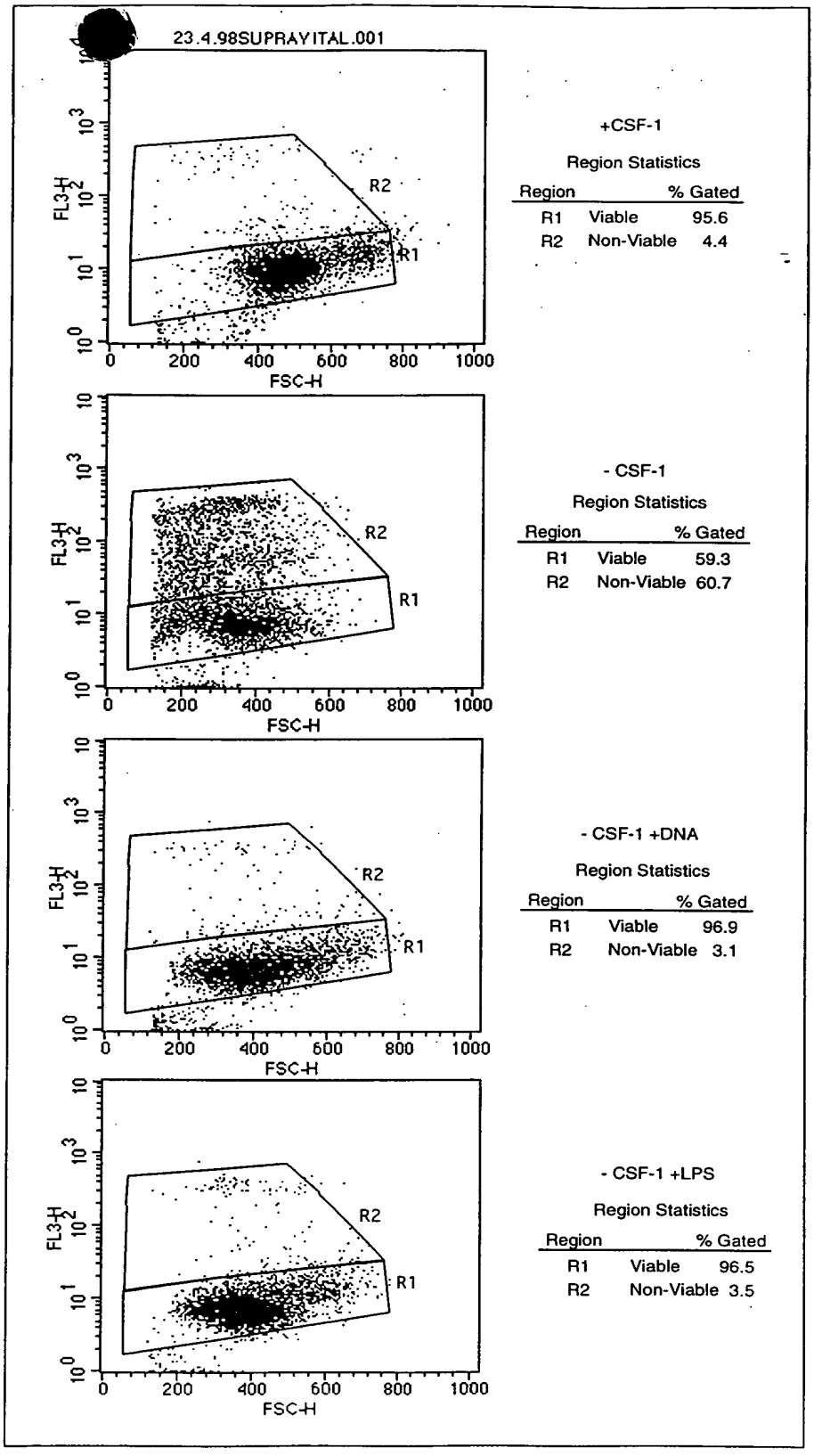
23.4.98SUPRAVITAL.001
FL3-H
FSC-H
R1
R2
+CSF-1
Region Statistics
Region % Gated
R1 Viable 95.6
R2 Non-Viable 4.4
- CSF-1
Region Statistics
Region % Gated
R1 Viable 59.3
R2 Non-Viable 60.7
- CSF-1 +DNA
Region Statistics
Region % Gated
R1 Viable 96.9
R2 Non-Viable 3.1
- CSF-1 +LPS
Region Statistics
Region % Gated
R1 Viable 96.5
R2 Non-Viable 3.5

FIGURE 3

FIGURE 4

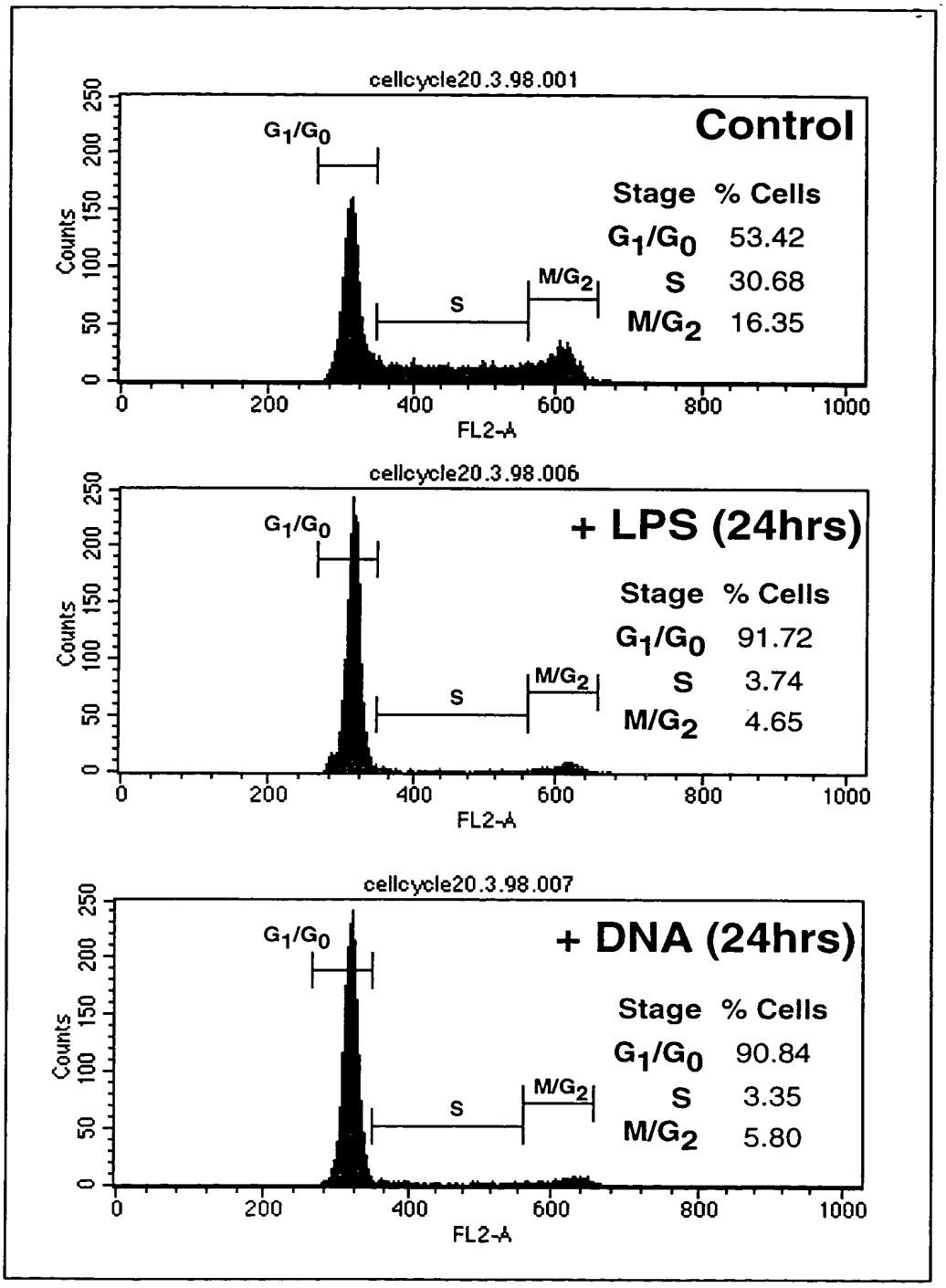
cellcycle20.3.98.001
Control
Stage % Cells
G1/G0 53.42
S 30.68
M/G2 16.35
G1/G0
S
M/G2
Counts
FL2-A
cellcycle20.3.98.006
+ LPS (24hrs)
Stage % Cells
G1/G0 91.72
S 3.74
M/G2 4.65
cellcycle20.3.98.007
+ DNA (24hrs)
Stage % Cells
G1/G0 90.84
S 3.35
M/G2 5.80

FIGURE 5A

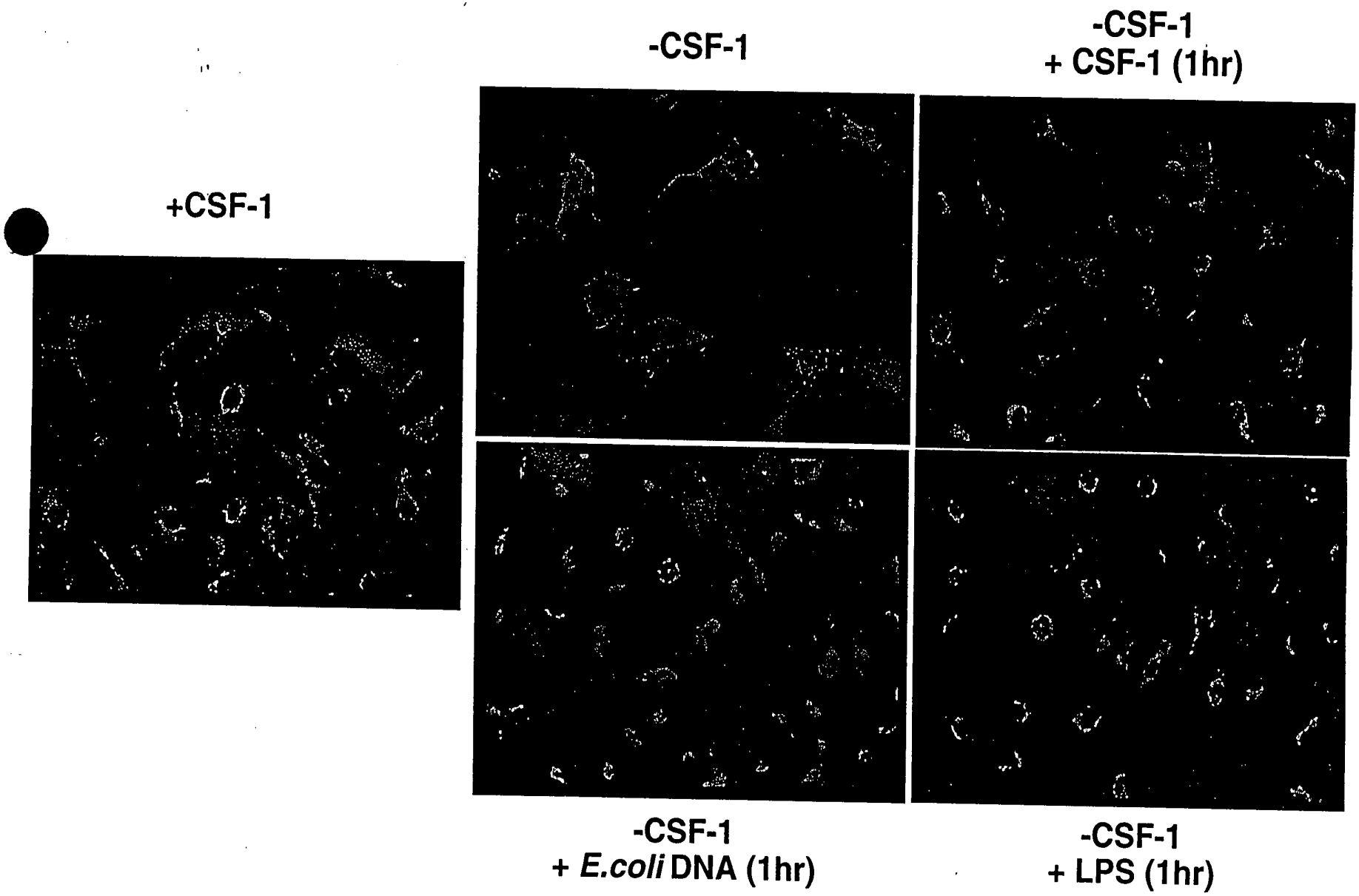

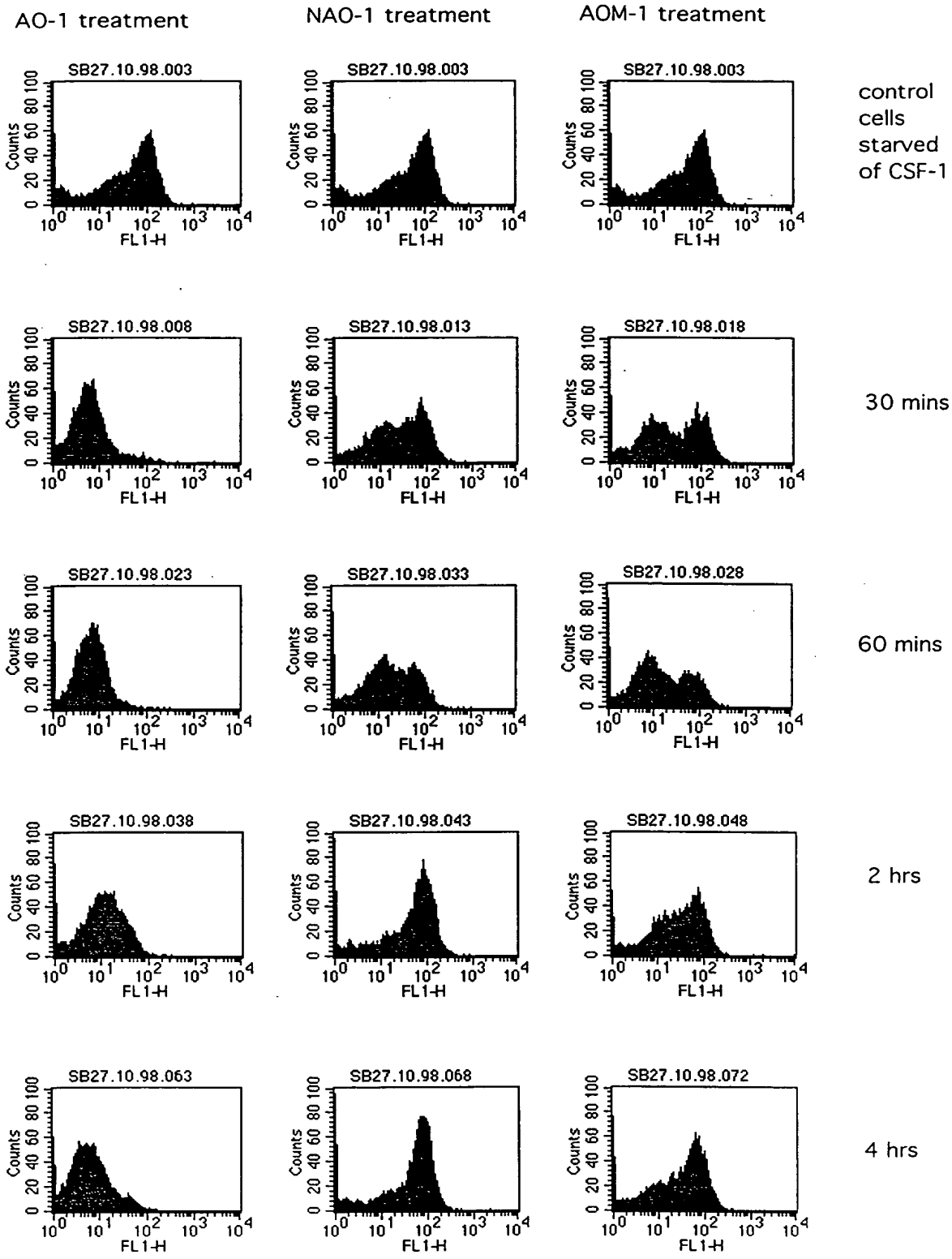
AO-1 treatment
NAO-1 treatment
AOM-1 treatment
SB27.10.98.003
SB27.10.98.003
SB27.10.98.003
control cells starved of CSF-1
SB27.10.98.008
SB27.10.98.013
SB27.10.98.018
30 mins
SB27.10.98.023
SB27.10.98.033
SB27.10.98.028
60 mins
SB27.10.98.038
SB27.10.98.043
SB27.10.98.048
2 hrs
SB27.10.98.063
SB27.10.98.068
SB27.10.98.072
4 hrs
Counts
FL1-H

FIGURE 5B

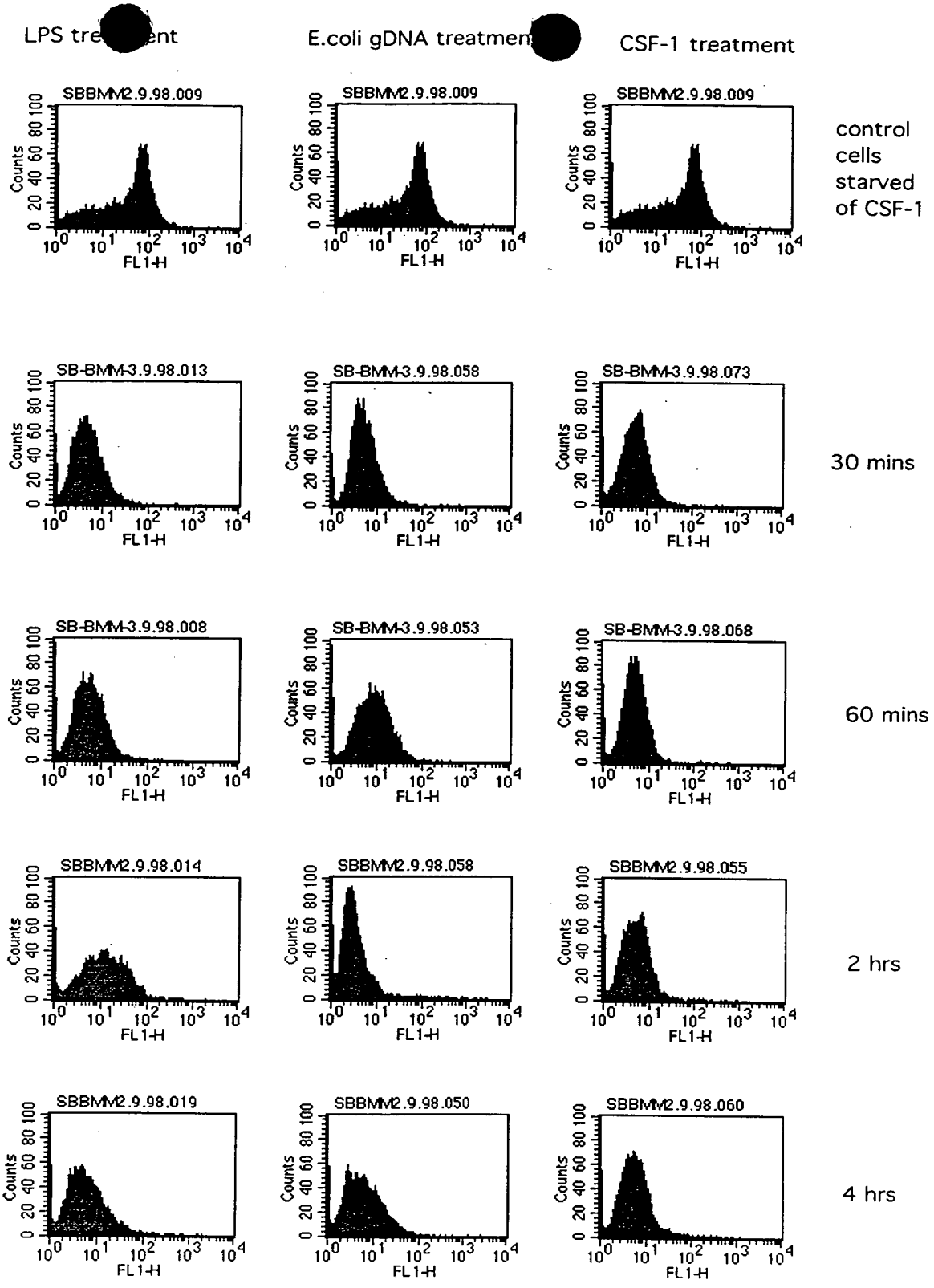

FIGURE 5B cont

FIGURE 6A

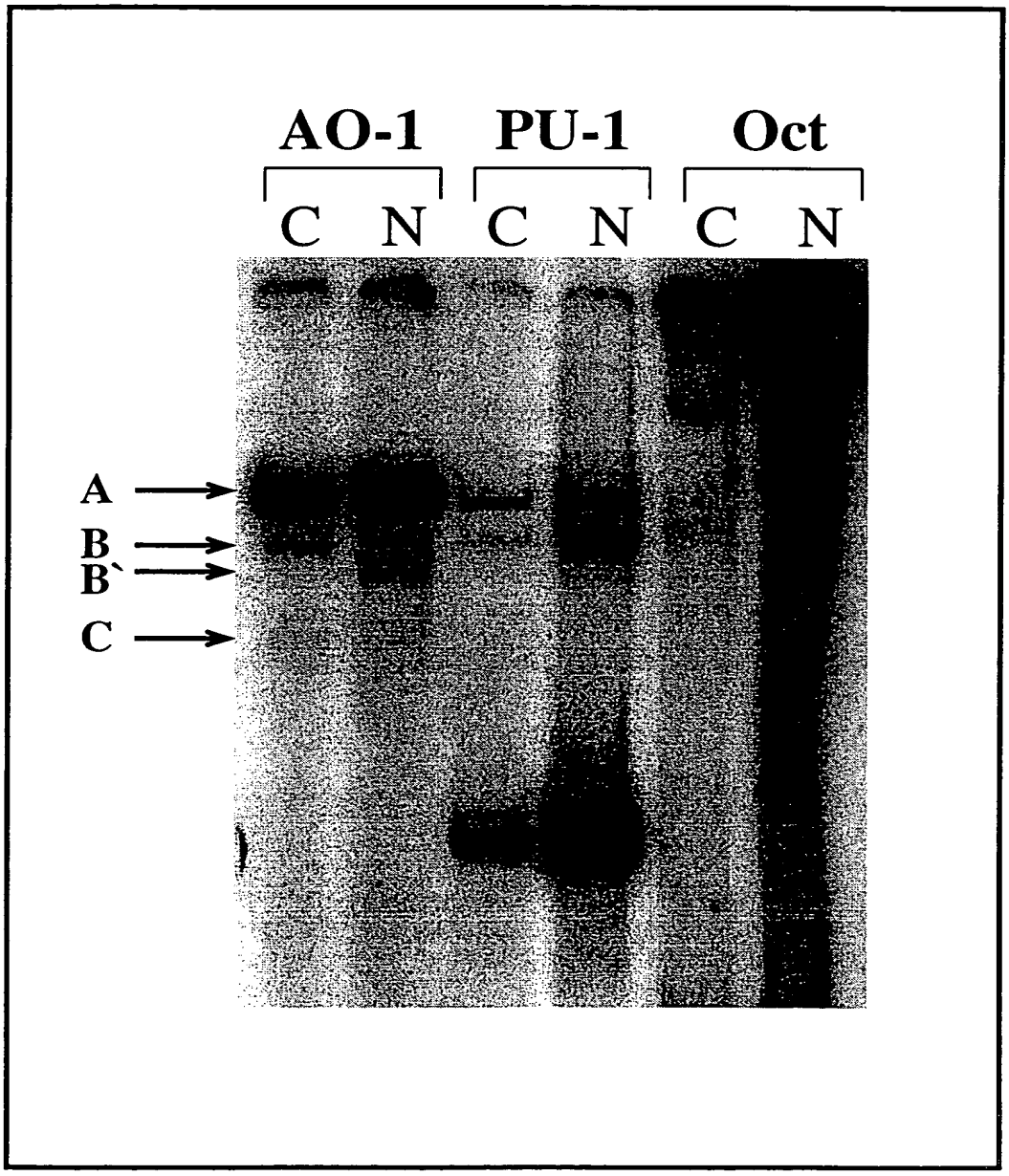

FIGURE 6B

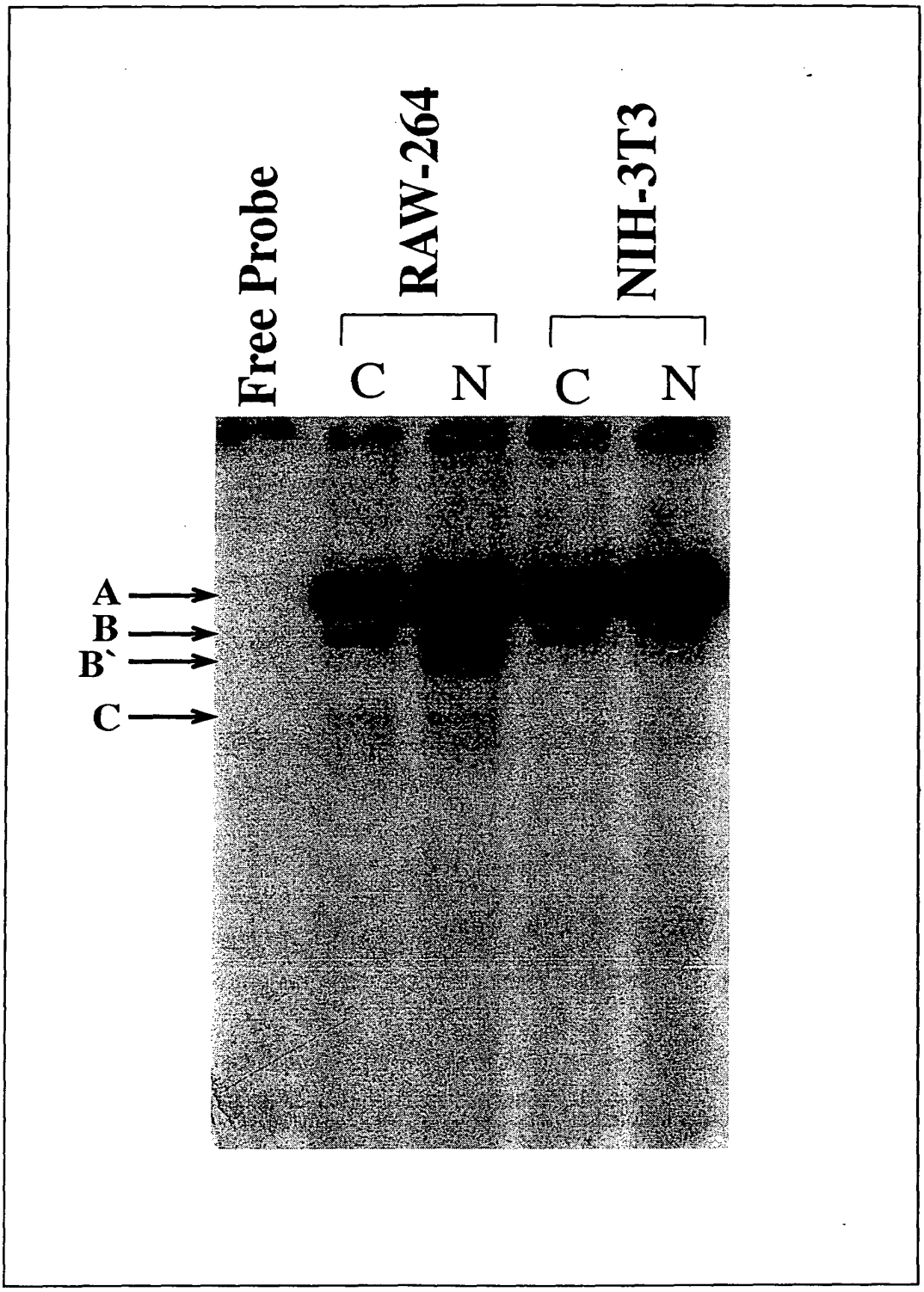

FIGURE 6C

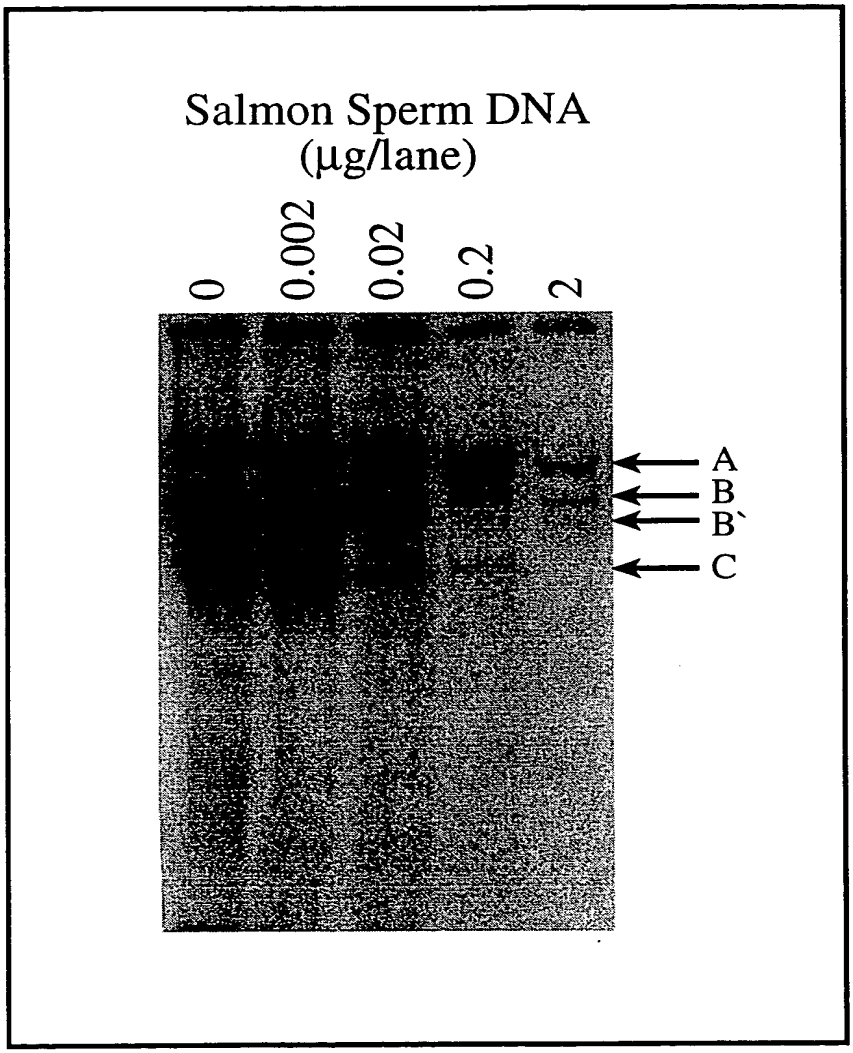

FIGURE 6D

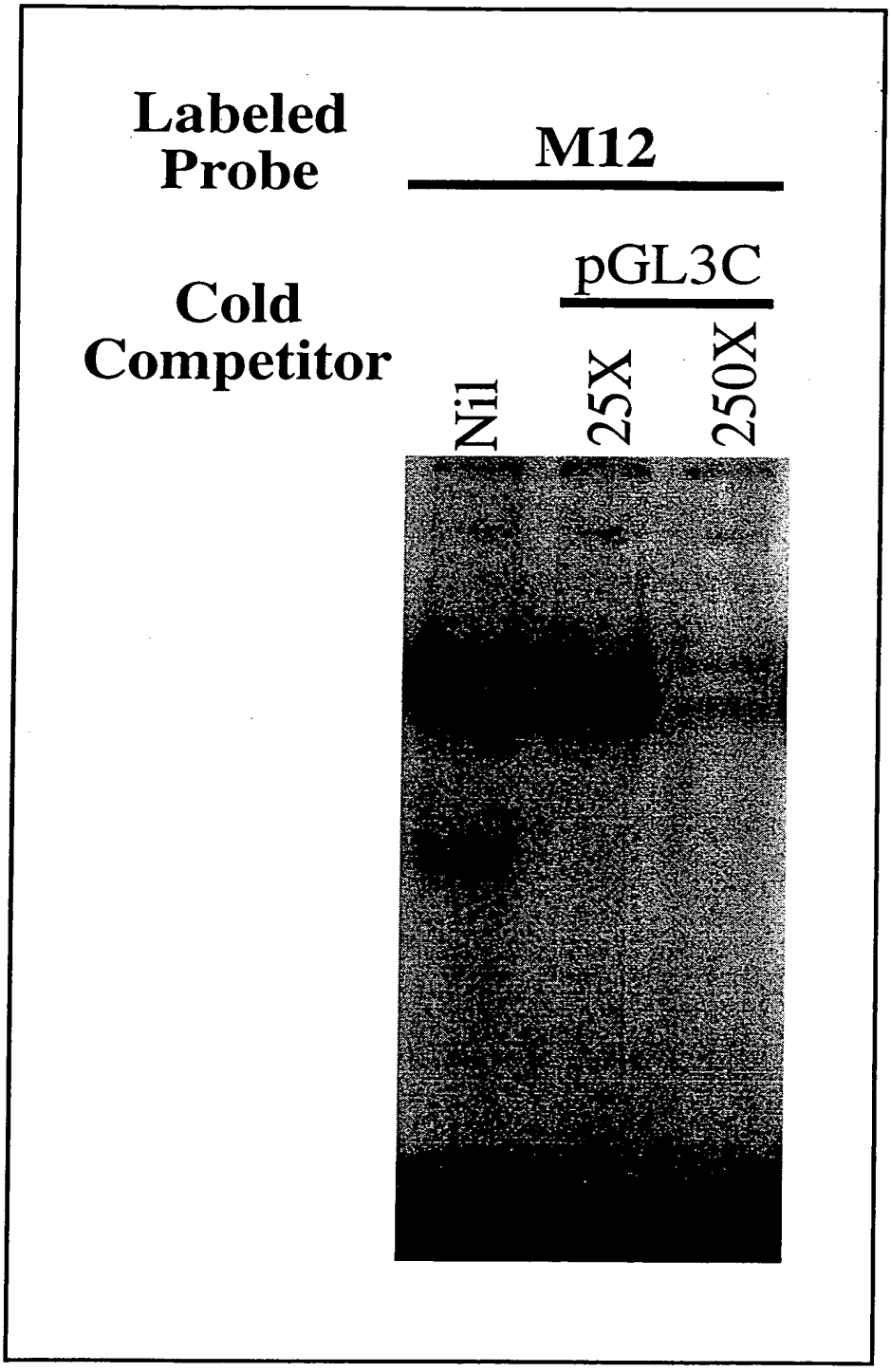

FIGURE 7A

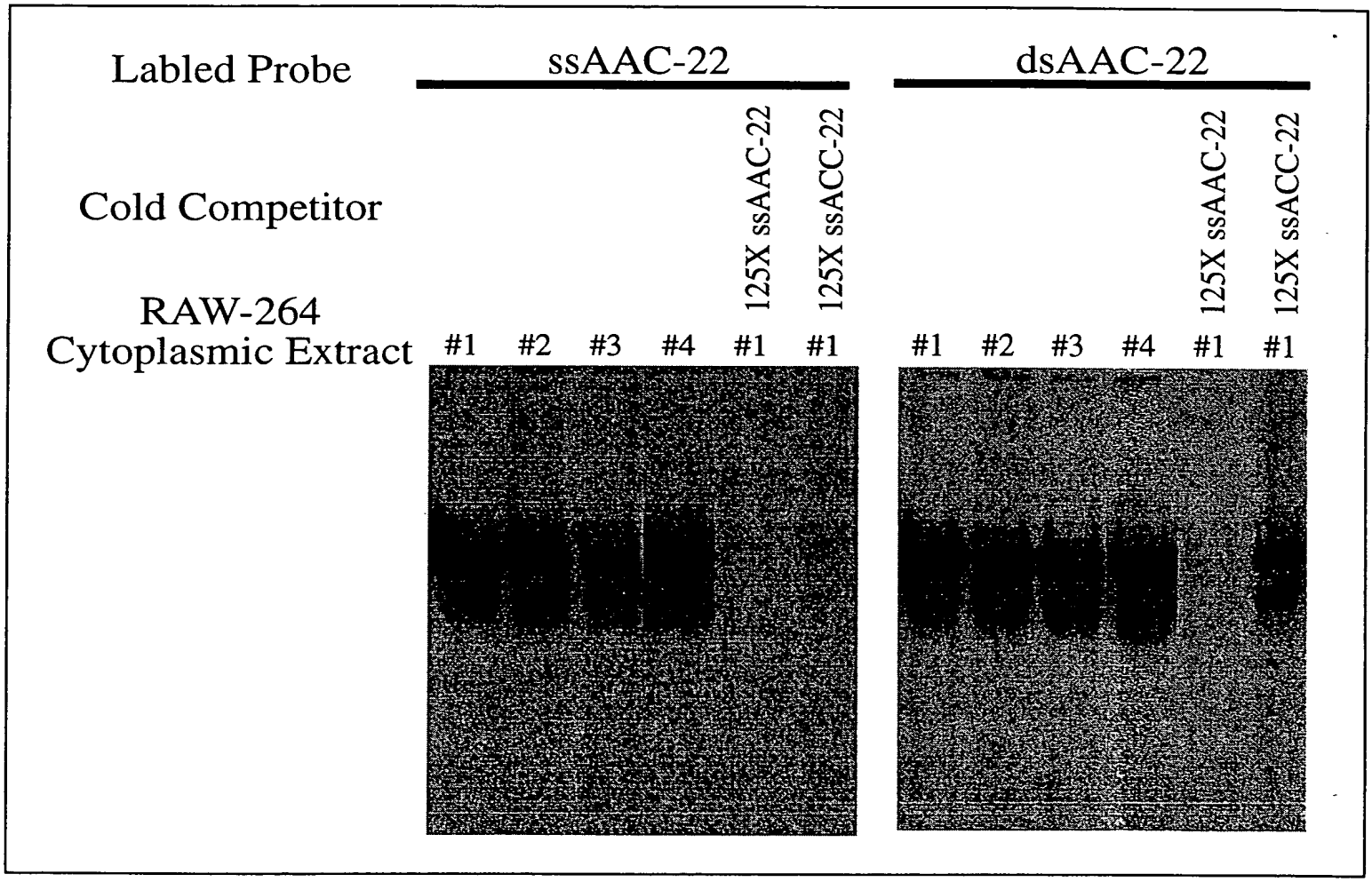
Labled Probe
ssAAC-22
dsAAC-22
Cold Competitor
125X ssAAC-22
125X ssACC-22
125X ssAAC-22
125X ssACC-22
RAW-264
Cytoplasmic Extract
#1
#2
#3
#4
#1
#1
#1
#2
#3
#4
#1
#1

FIGURE 7B

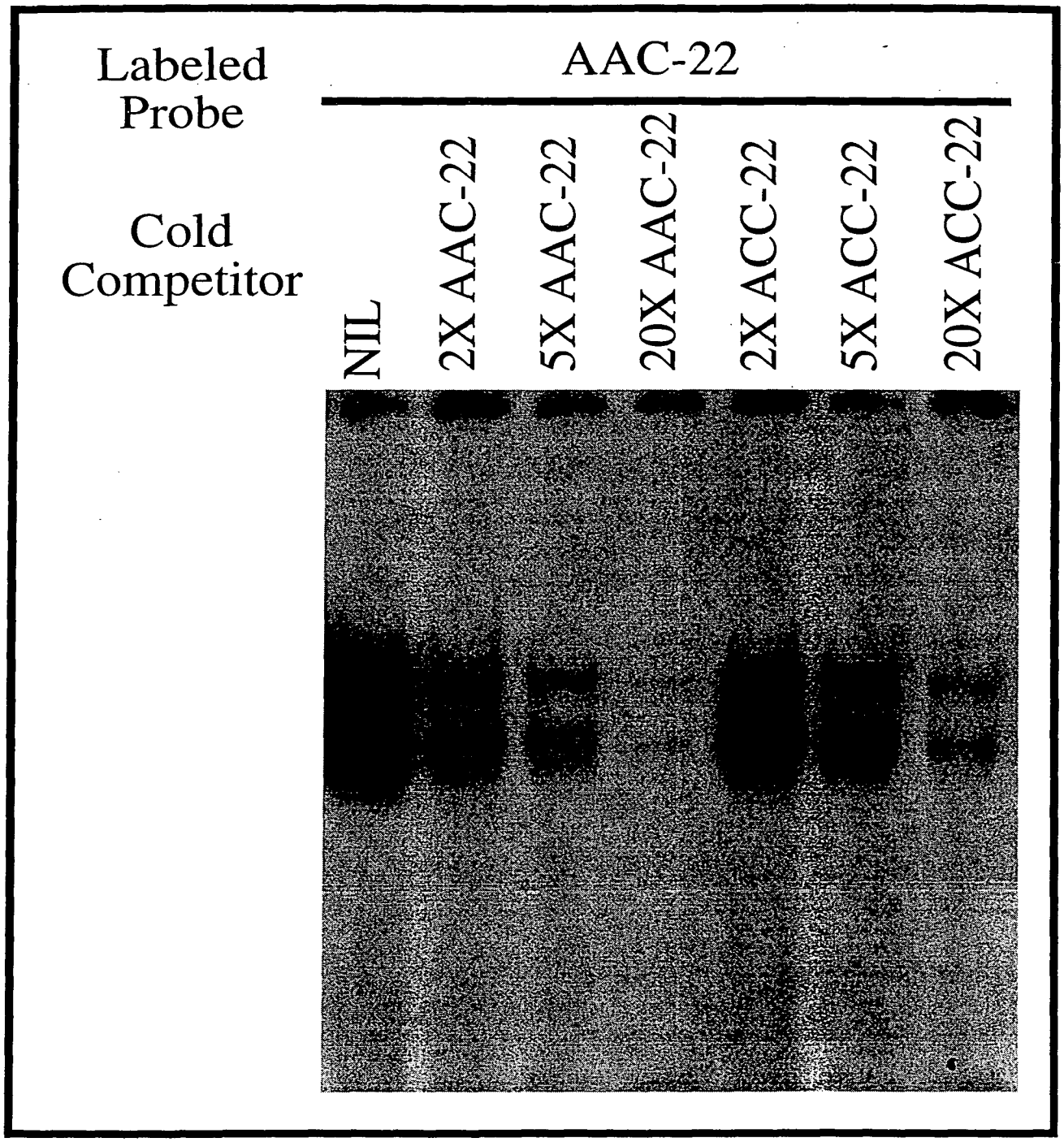
Labeled Probe
AAC-22
Cold Competitor
NIL
2X AAC-22
5X AAC-22
20X AAC-22
2X ACC-22
5X ACC-22
20X ACC-22

FIGURE 7C

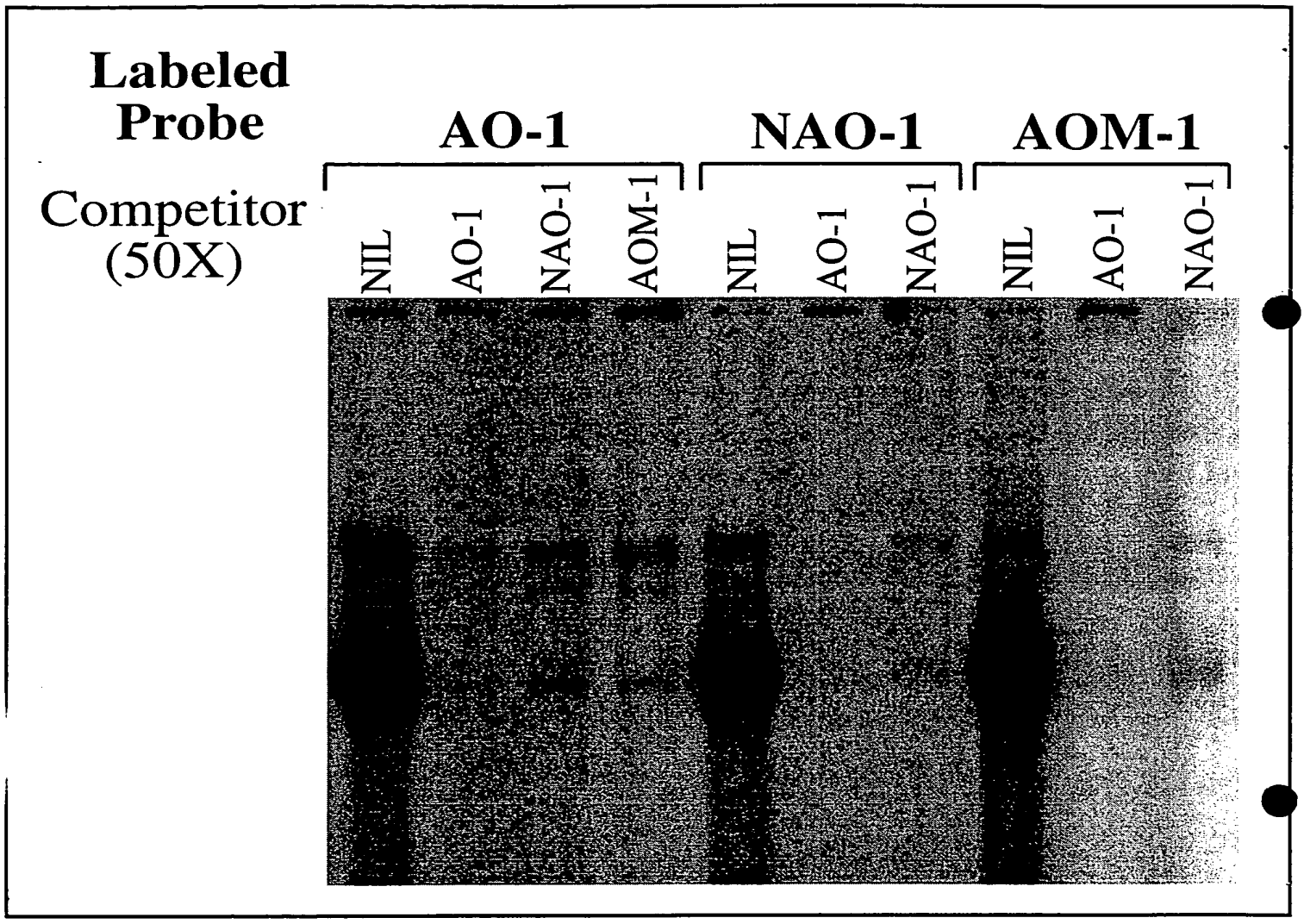
Labeled Probe
AO-1
NAO-1
AOM-1
Competitor (50X)
NIL
AO-1
NAO-1
AOM-1
NIL
AO-1
NAO-1
NIL
AO-1
NAO-1

FIGURE 7D

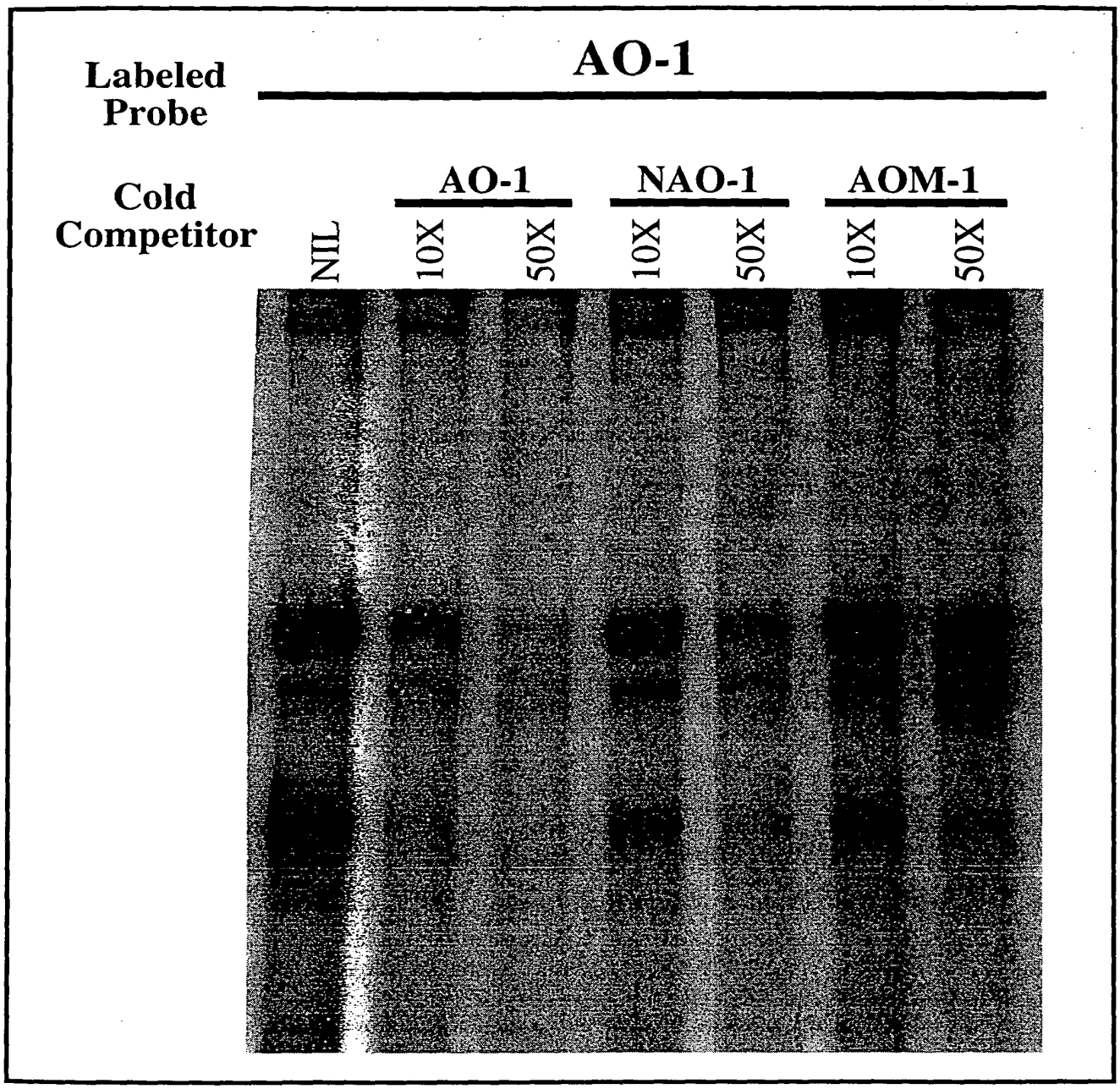
Labeled Probe
AO-1
Cold Competitor
AO-1
NAO-1
AOM-1
NIL
10X
50X
10X
50X
10X
50X

FIGURE 7E

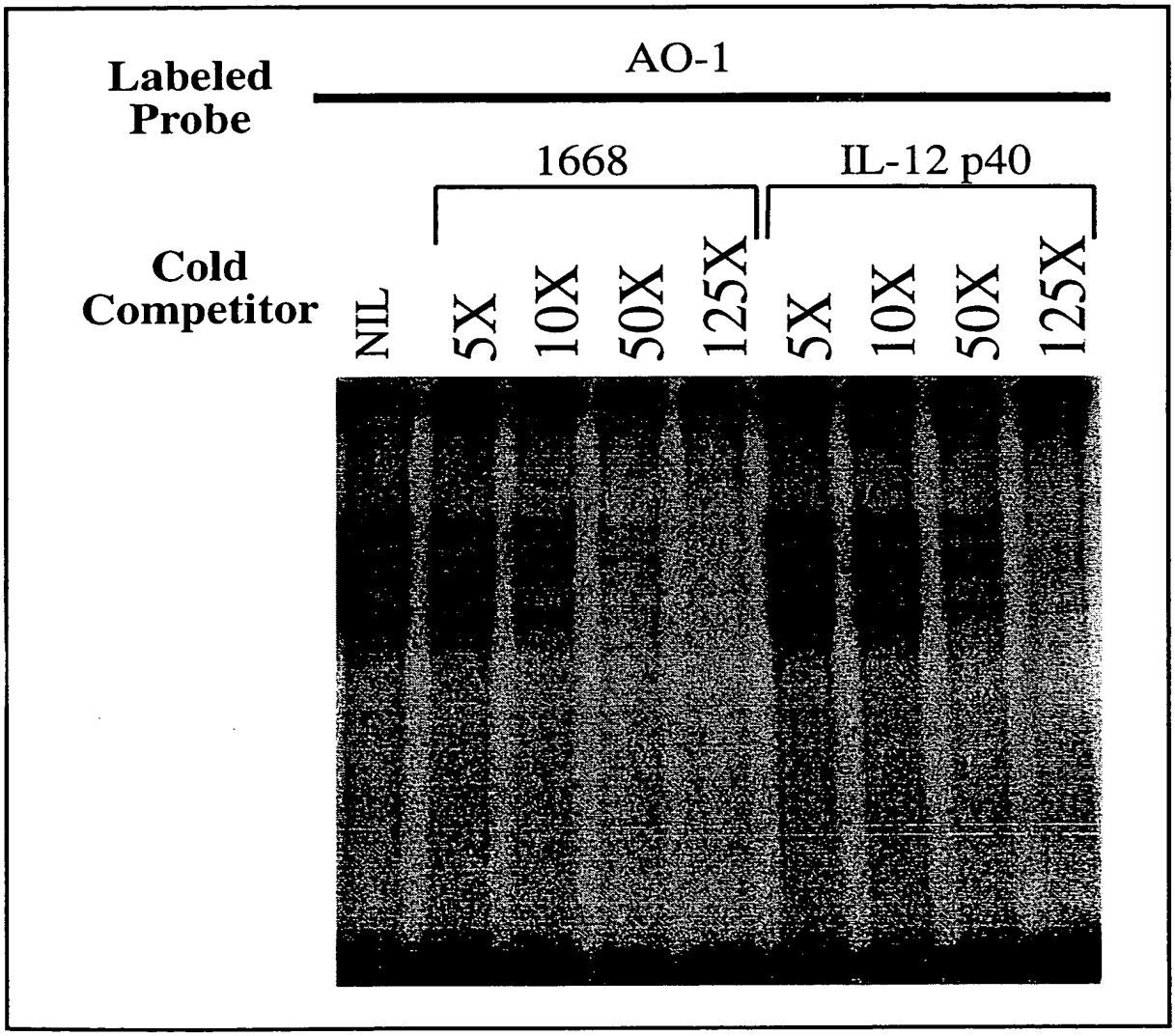
Labeled Probe
AO-1
1668
IL-12 p40
Cold Competitor
NIL
5X
10X
50X
125X
5X
10X
50X
125X

FIGURE 8A

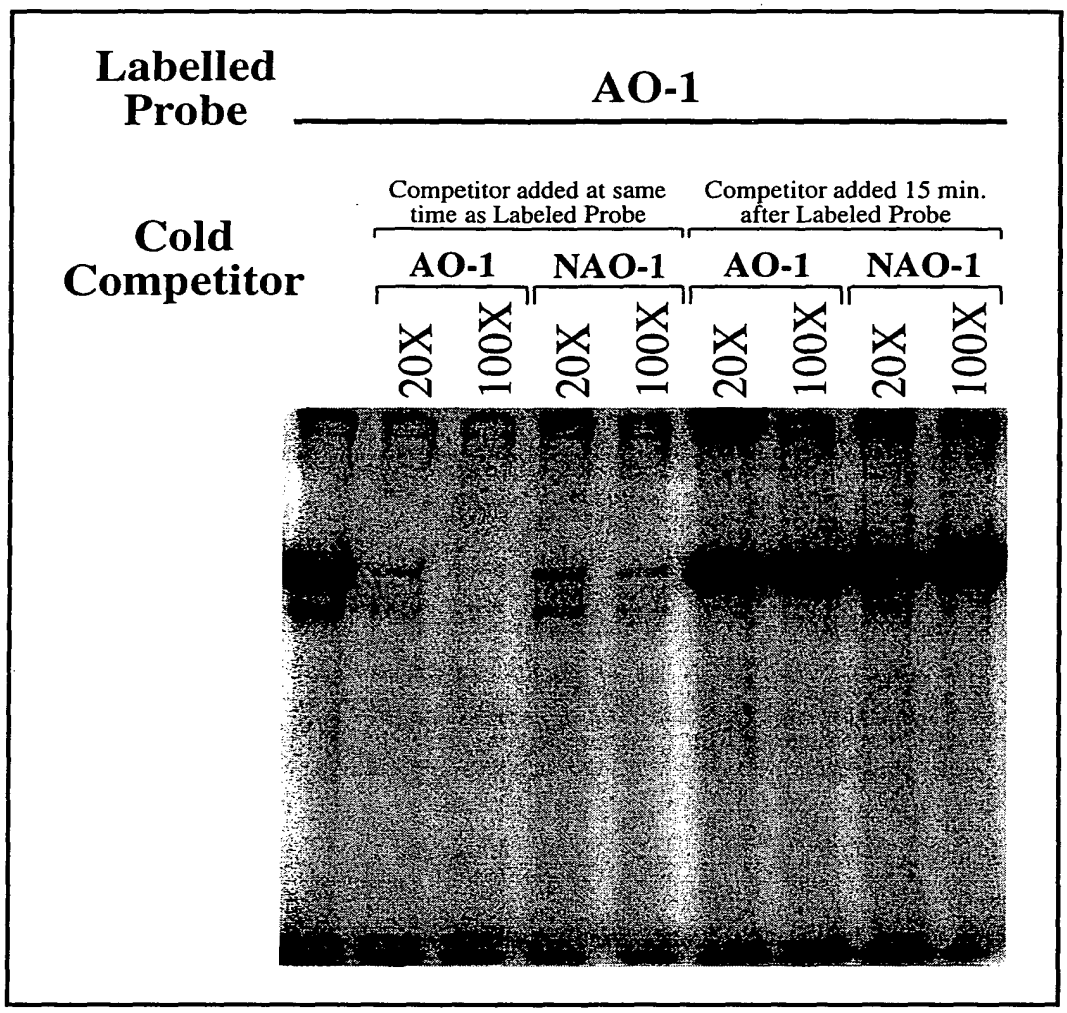
Labelled Probe
AO-1
Cold Competitor
Competitor added at same time as Labeled Probe
Competitor added 15 min. after Labeled Probe
AO-1
NAO-1
AO-1
NAO-1
20X
100X
20X
100X
20X
100X
20X
100X

FIGURE 8B

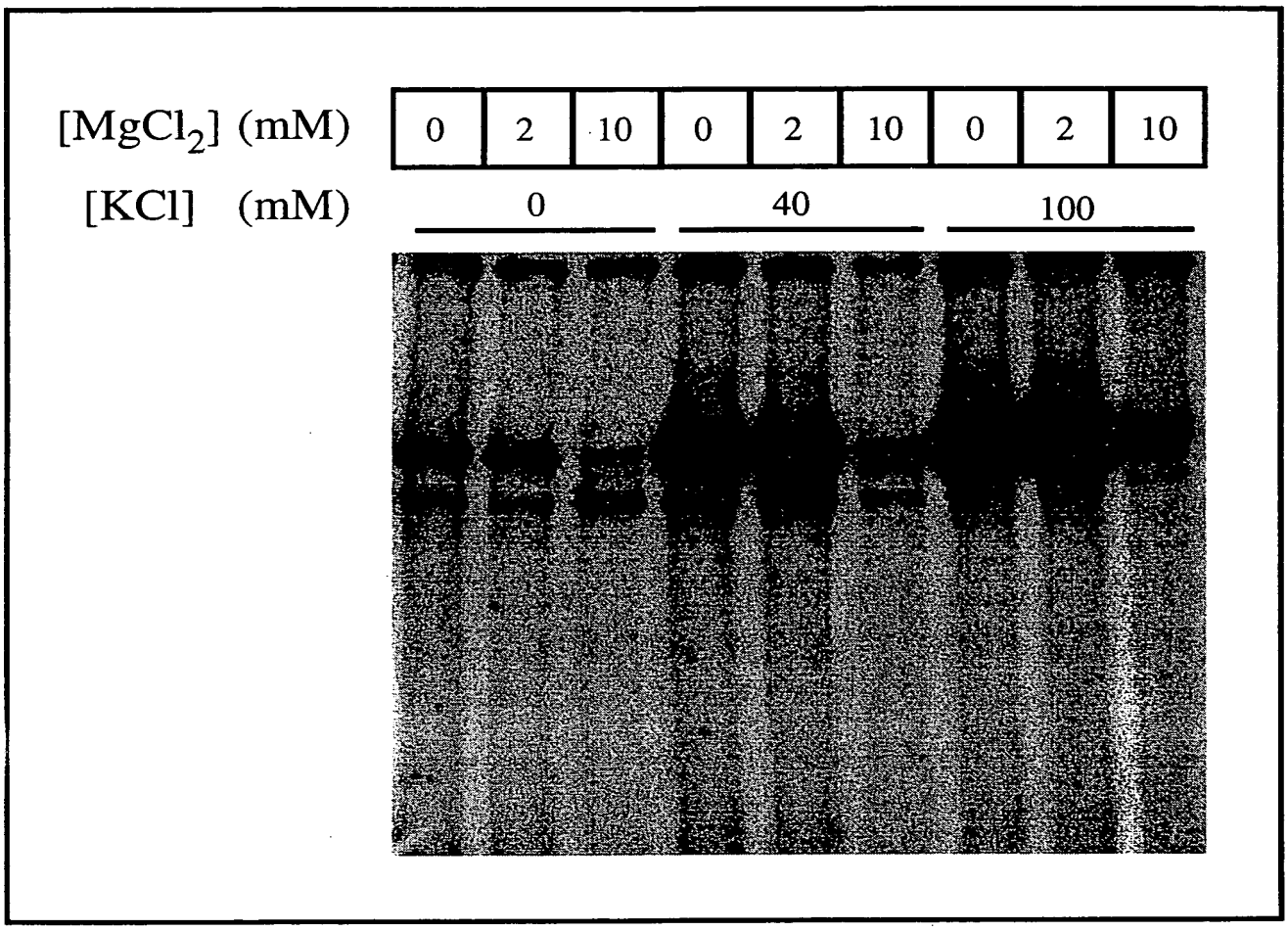

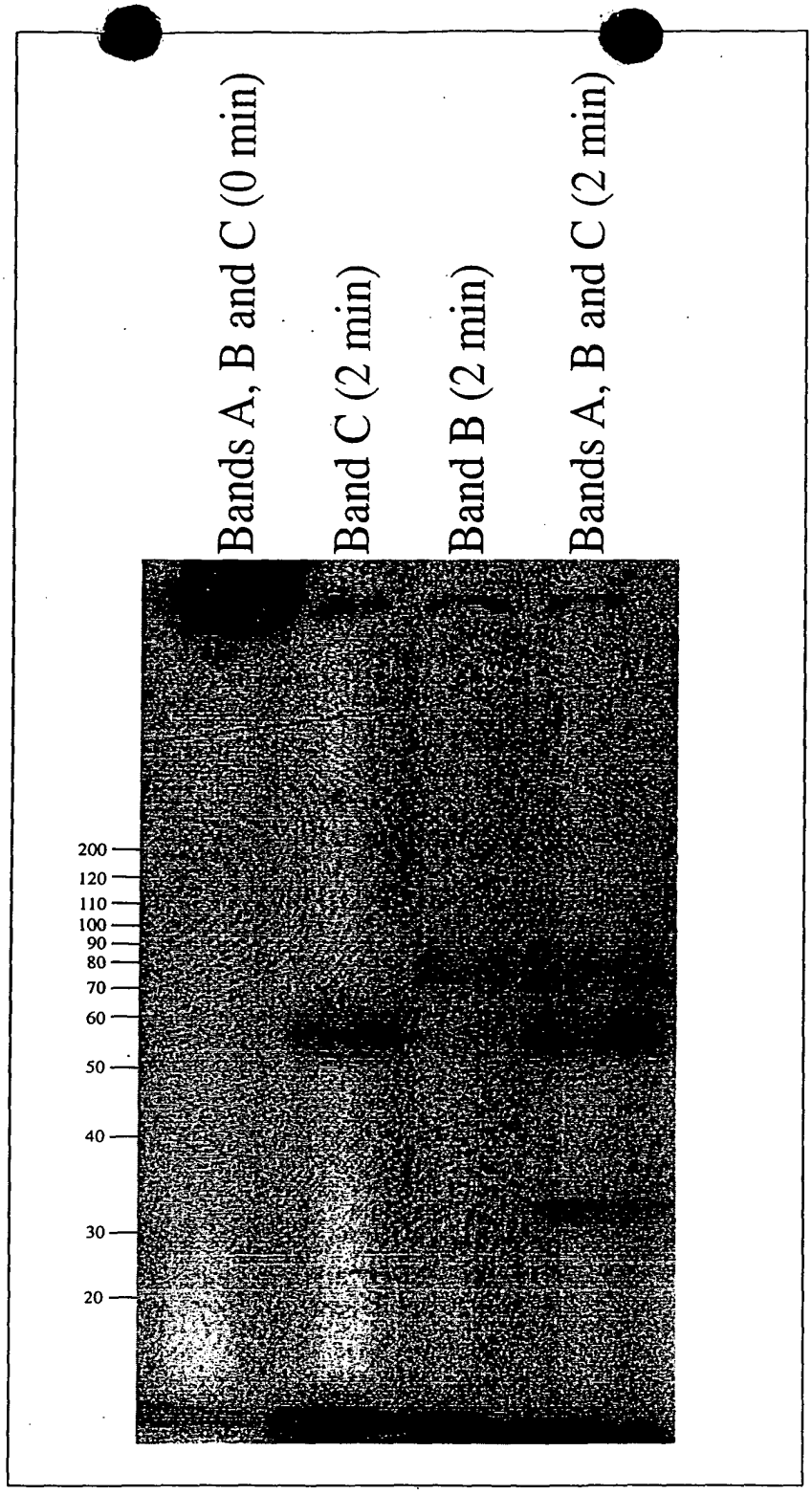
Bands A, B and C (0 min)
Band C (2 min)
Band B (2 min)
Bands A, B and C (2 min)
200
120
110
100
90
80
70
60
50
40
30
20

FIGURE 9

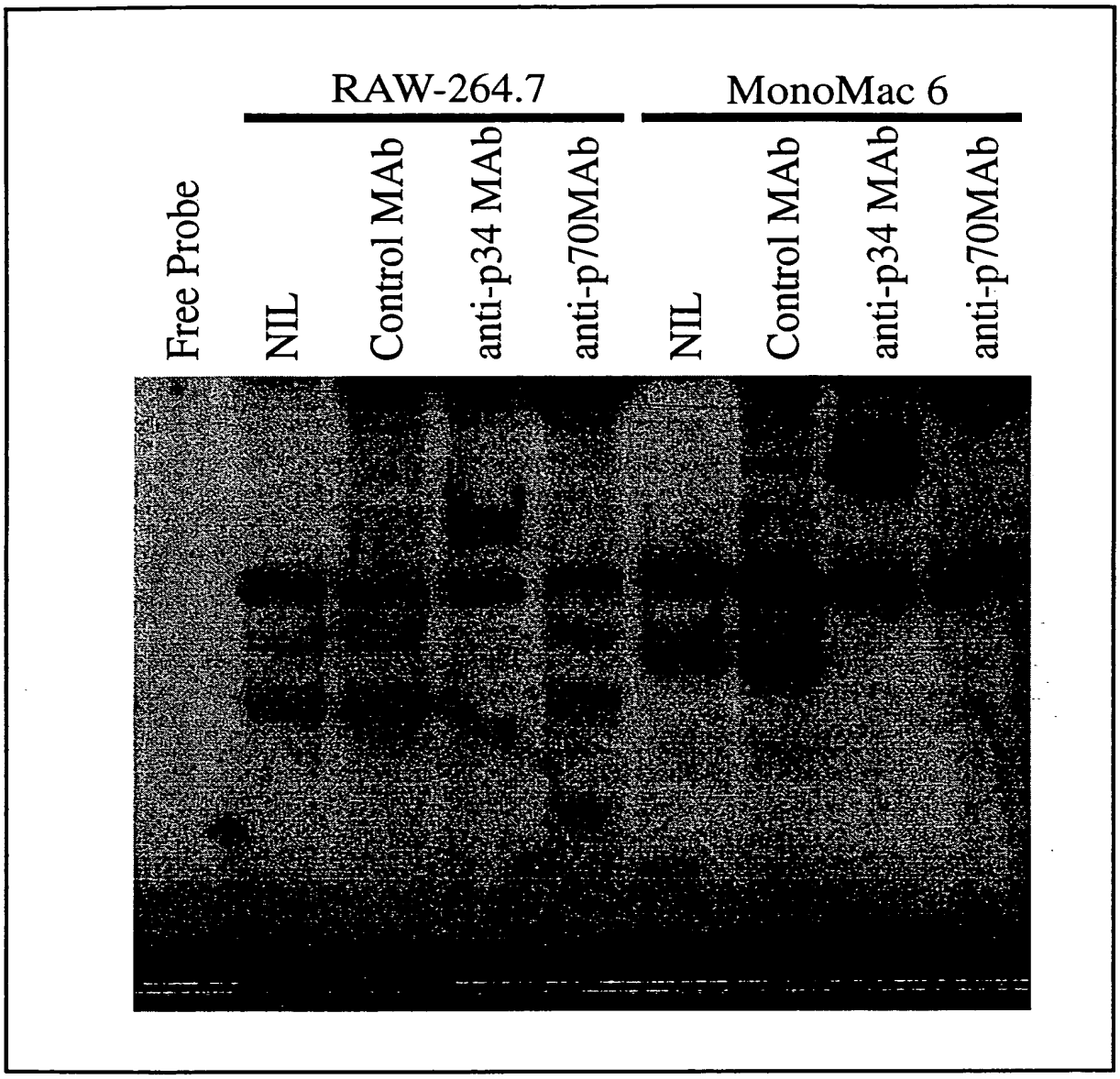
RAW-264.7
MonoMac 6
Free Probe
NIL
Control MAb
anti-p34 MAb
anti-p70MAb
NIL
Control MAb
anti-p34 MAb
anti-p70MAb

FIGURE 10